

**DESIGN OF IN-VITRO OPTICALLY AIDED ROBOTIC
MANIPULATION (IVOARM)**

CHIA KOK SIANG

**A project report submitted in partial fulfilment of the
requirements for the award of the degree of
Bachelor (Hons.) of Mechatronics Engineering**

**Faculty of Engineering and Science
Universiti Tunku Abdul Rahman**

May 2011

DECLARATION

I hereby declare that this project report is based on my original work except for citations and quotations which have been duly acknowledged. I also declare that it has not been previously and concurrently submitted for any other degree or award at UTAR or other institutions.

Signature : _____

Name : Chia Kok Siang

ID No. : 0807UEB099

Date : _____

APPROVAL FOR SUBMISSION

I certify that this project report entitled “DESIGN OF IN-VITRO OPTICALLY AIDED ROBOTIC MANIPULATION (IVOARM)” was prepared by CHIA KOK SIANG has met the required standard for submission in partial fulfilment of the requirements for the award of Bachelor of Engineering (Hons.) Mechatronics at Universiti Tunku Abdul Rahman.

Approved by,

Signature : _____

Supervisor : Dr. Tan Ching Seong

Date : _____

The copyright of this report belongs to the author under the terms of the copyright Act 1987 as qualified by Intellectual Property Policy of Universiti Tunku Abdul Rahman. Due acknowledgement shall always be made of the use of any material contained in, or derived from, this report.

© 2011, Chia Kok Siang. All right reserved.

ACKNOWLEDGEMENTS

First of all, I would like to express my gratitude to everyone who has contributed their help and funds, directly or indirectly. Here, I would like to thank Dr Tan Ching Seong for his invaluable guidance and advice in helping me to have more understanding in this project. Besides that, his encouragement and support has inspired me in completing this project.

Other than that, I would also like to thank Mr Goh Han Cheong, an engineer cum director of IPE Automation Sdn. Bhd. who has helped me in giving his expertise and guided me in going through all the industrial manufacturing process. With his professional guidance and years of experience in industry, he has cut short my time in manufacturing process as well as solving the manufacturing problem.

Besides that, we would like to express my gratitude to Agilent Instrument Company who has provided technical support and equipment to us to complete this project.

Lastly but not least, I would like to thank Universiti Tunku Abdul Rahman for giving me a chance to do this project.

IN-VITRO OPTICALLY AIDED ROBOTIC MANIPULATION (IVOARM)

ABSTRACT

In-Vitro Optically Aided Robotic Manipulation (IVOARM) constitutes a blind grasping concept using two anthropomorphic fingers with the aid of the directional force sensors and infrared sensors mounted on it. This manipulator is controlled by an embedded system with high DSP compatibility. The infrared sensors are mounted on the surface of the finger gripper to detect the presence of the object in the area of the grasping. The physical information of the object such as size and centroid of the object is determined using the algorithm developed with the aid by the infrared sensors. The purpose of determining the centroid is to determine the size and method to grasp the object. The result of the object size determination using the IVOARM has been obtained.

Based on the size of the object obtained from the calculation, the object will be decided to be gripped in either full envelope gripping or finger tip gripping. Force will be calculated to ensure proper force to be applied.

TABLE OF CONTENTS

DECLARATION	ii
APPROVAL FOR SUBMISSION	iii
ACKNOWLEDGEMENTS	v
ABSTRACT	vi
TABLE OF CONTENTS	vii
LIST OF TABLES	xi
LIST OF FIGURES	xiii
LIST OF SYMBOLS / ABBREVIATIONS	xviii
LIST OF APPENDICES	xix

CHAPTER

1	INTRODUCTION	20
	1.1 Background	20
	1.2 Aims and Objectives	21
	LITERATURE REVIEW	22
	2.1 Robot Grasping of Unknown objects, Description and Validation of the Function with Quadriplegic People	23
	2.1.1 Flow chart	24
	2.1.2 Distance Estimation	24
	2.1.3 Feature extraction	25
	2.1.4 Matching and localization	25
	2.1.5 Evaluation	27
	2.2 High Performance Robotic Gripper Based on Choice of Feedback Variables	27

2.2.1	Mechanical design	28
2.2.2	Sensors	28
2.2.3	Evaluation	28
2.3	Design and Construction of a Robotic Gripper for Activities of Daily Living for People with Disabilities	29
2.3.1	Mechanical Design	30
METHODOLOGY		33
MECHANICAL DESIGN		41
4.1	Engineering Design	41
4.1.1	The need identification and problem definition	42
4.1.2	Design Requirement	42
4.1.3	Conceptual Design	42
4.1.4	Concept Theory	45
4.1.5	Embodiment Design	47
4.1.6	Virtual Design in SolidWork	54
4.1.7	Detailed Modelling	63
4.1.8	CAD Drawing Sent to Manufacturer.	66
4.1.9	Feedback from the Manufacturer	68
4.1.10	Pocket Hole	68
4.1.11	Bearing Housing	68
4.1.12	Palm	69
4.1.13	Screw hole	69
4.1.14	CAD Drawing	70
4.1.15	Dowel pin.	71
4.2	Assembly of Component Parts	71
4.3	Test and Validate Through Experiment	74
4.3.1	Overview of the Mechanical Design Experiment	74
4.3.2	Experiment Method	75
4.3.3	Maximum Force at Tips	76
5.1	Overview of the Sensor Development Experiment	79
5.2	Infrared Sensors Development	80

5.2.1	Location of Infrared sensors	80
5.2.2	Beyer's Polygon Area	80
5.3	The Accuracy of Servomotor's Angle of Turning Relatives to Infrared Object Detector	83
5.4	Force Sensor Development	84
5.4.1	Force Response	84
5.4.2	Experiment on Specimens	84
5.4.3	Experiment on Force Sensors' Response.	85
5.5	Experiment on the FSR's voltage output level relative to the location it locates in the gripper's finger.	86
6	RESULTS AND DISCUSSIONS	88
6.1	Mechanical Design	88
6.1.1	Body Part Weight	88
6.2	Result on Pattern Grasping	89
6.3	Sensors Development	93
6.3.1	Experiment on Location of Sensors	93
6.4	Servomotor's angle's of turning relative to the IROD detection range on the object's surface	95
6.5	Force Sensor's Development	96
6.5.1	Experiment of Force Applied on Specimen	96
6.5.2	Experiment on Force Sensors	99
6.5.3	Force Respond on Each Location of the FSR	101
7	DISCUSSION ON ENGINEERING DESIGN PROCESS	103
7.1.1	Pocket Hole	103
7.1.2	Bearing Housing	104
7.1.3	Palm	105
7.1.4	Screw hole	105
7.1.5	CAD Drawing	106
7.1.6	Dowel pin.	107
7.1.1	IRDD sensors location and offset in palm	108
7.1.2	Gripper's finger Vibration	108

7.1.3	L-shape plate to fix position	109
7.1.4	Position of Force Sensor	110
7.1.5	Offsetting the position of IRDD into the palm	111
7.1.6	The Grasping at Finger Tip Subjects to Rotational Force	112
7.1.7	Publication in symposium	112
8	CONCLUSION AND RECOMMENDATIONS	113
8.1	Conclusion	113
8.1.1	Mechanical Design	113
8.1.2	Sensors Development	113
8.2	Recommendation	114
8.2.1	Dynamic Force Control	114
8.2.2	Slip sensing	114
8.2.3	Determine the Volume of the object	114
8.2.4	Torque Increment	115
8.3	Precaution	115
8.3.1	Servomotor	115
8.3.2	Wiring	115
8.3.3	Complete wiring connection between IVOARM and circuit board.	115
	REFERENCES	116
	APPENDICES	118

LIST OF TABLES

TABLE	TITLE	PAGE
	Table 1: Evaluation on each of the grippers with IVOARM	32
	Table 2: List of hardware	39
	Table 3: Comparison of conceptual designs	43
	Table 4: Comparison of Infrared Object Detector TCRT family series	48
	Table 5: Comparison of Motor	49
	Table 6: Comparison of Ultrasonic Range Finder and the SHARP GP2D120.	50
	Table 7 Comparison of Force Sensors' Characteristic	51
	Table 8: The finger body location and length	56
	Table 9: The stress concentration location with force applied.	65
	Table 10: David-Hartenberg Table	77
	Table 11: Comparison between actual weight and simulated weight in Solidwork	88
	Table 12: Experiment result on spring	90
	Table 13: Force experiment result on finger thumb	91

Table 14: The calculated area of sensing of the Infrared sensors relative to the location chosen	93
Table 15: The simulated area of Sensing of the Infrared Sensors relative to the location chosen	93
Table 16: Experiment on servomotors' angle of turning relative to IROD's detection on different object's position at dim room	95
Table 17: Simulated of Servomotor's angle of turning relative to IROD's detection on different	95
Table 18: Experiment of Force Sensor Resistor on Different Load	99
Table 19: The force sensors output voltage and force respond on can grasping	102

LIST OF FIGURES

FIGURE	TITLE	PAGE
Figure 2.1:	The flow chart on the MADEUS operation (Adopted from Christophe Leroux, et al, 2007)	24
Figure 2.2:	The flow chart on the MADEUS operation (Adopted from Christophe Leroux, et al, 2007)	25
Figure 2.3:	The matching and localization (Adopted from Christophe Leroux, et al, 2007)	26
Figure 2.2.4:	The mechanical design of the HPRG gripper (adopted from Christophe Leroux, et al, 2007)	27
Figure 2.5:	Manus gripper internal mechanical part (adopted from Redwan Alqasemi, et al, 2007)	29
Figure 2.6:	Manus gripper internal mechanical part (adopted from Redwan Alqasemi, et al, 2007)	30
Figure 2.7:	Various finger tip of the Manus Gripper (adopted from Redwan Alqasemi, et al, 2007)	31
Figure 3.1:	The flow chart of Engineering Design	33
Figure 3.2:	Flowchart sensor development	34
Figure 3.3:	POLC process flow	36
Figure 3.4:	Project Gantt chart, colour indicate time to planned schedule to complete the tasks and black line indicates total period to complete a sub system	38
Figure 3.5:	List of virtual designs drawn in SolidWorks	40
Figure 4.1:	Comparison of various conceptual designs.	44
Figure 4.2:	Kinematic of gripper	46

Figure 4.3: Non-self intersecting planar to calculate determinant. (adopted from Eric Weisstein, 2011)	47
Figure 4.4: The layer structure of force sensors	51
Figure 4.5 The bearing for the joint of IVOARM	52
Figure 4.6: The dowel pin	52
Figure 4.7: The motor coupler	53
Figure 4.8: Interface of the SolidWorks program.	54
Figure 4.9: Labeling of common features of all the finger body	55
Figure 4.10: The dimension specification of the Servomotor Hitec HS-56	55
Figure 4.11: The minimum dimension of the finger body in front view and top view.	56
Figure 4.12: The assignment of name for each of the finger bodies.	56
Figure 4.13: The pocket hole for the infrared object detector is circle at the thumb finger.	57
Figure 4.14: The bearing housing designed at the base of the finger body.	57
Figure 4.15: The coupler housing housed with a coupler	58
Figure 4.16: The radius fillet at the edge of finger body.	58
Figure 4.17: The view of palm design	59
Figure 4.18: The extruded linear line at base at 35m	59
Figure 4.19: The foundation settlement in virtual display	60
Figure 4.20: Top view of the three joint finger part.	60
Figure 4.21: Side view of the three joint finger gripper parts	61
Figure 4.22: Side view of the two joint finger gripper parts.	61
Figure 4.23: Top view of two joints finger	61
Figure 4.24: Top view of the palm of the IVOARM gripper	62

Figure 4.25: Side view of the palm of the IVOARM gripper.	62
Figure 4.26: Full assembly of IVOARM gripper with foundation settlement in virtual form	62
Figure 4.27: The workspace of the Gripper finger IVOARM in Solidwork software.	63
Figure 4.28: The stress concentration on the surface of the finger gripper A	64
Figure 4.29: The stress concentration on the surface of the finger gripper B	64
Figure 4.30: The stress concentration on the surface of the finger gripper C	64
Figure 4.31: The stress concentration on the surface of the thumb	65
Figure 4.32: The stress concentration on the surface of the finger tip	65
Figure 4.33: Bill of material of the IVOARM gripper	66
Figure 4.34: The CAD drawing of the Joint_finger tip	67
Figure 4.35: Exploded view of the IVOARM	67
Figure 4.36: The Mickey Mouse hole drilled at the pocket holes	68
Figure 4.37: The new location of the bearing	69
Figure 4.38: The new bearing housing location view in 3 Dimension.	69
Figure 4.39: The CSK screw hole that support the servomotor with finger body	70
Figure 4.40: Two 'U' shape palm with different labelling	70
Figure 4.41: The thin rod dowel pin on the left side and the dowel pin with angle on right side	71
Figure 4.42: The assembly step by step of IVOARM	74
Figure 4.43: Experiment on spring to obtain the constant, k.	75
Figure 4.44: Spring is subject to elongation from the rotation of the gripper's finger which pulls the spring.	75

Figure 4.45: The spring is measured to determine the force at tip.	76
Figure 4.46: Angle is taken as the same time with measurement of spring at tip	76
Figure 4.47: The kinematic of three joint to formulate static force and torque propagation	76
Figure 5.1: The experiment flow chart for the Sensor Development	79
Figure 5.2: The actual sensing points of the IROD and the IRDD in IVOARM	81
Figure 5.3: Simulation result on angle of rotation. The IROD sensing range is fixed.	84
Figure 5.4: The INSTRON 5582 machine used to test the maximum force onto specimens	85
Figure 5.5: The surface of the FSR which is reinforced with the rubber pad.	86
Figure 5.6: The experiment of getting FSR individual force response. FSR is applied with a load.	86
Figure 5.7: The joint's number and the sensor's location.	87
Figure 5.8: The experiment on grasping an object and measuring the FSR force response.	87
Figure 6.1: Comparison between simulated grasping pattern and the experimental grasping pattern	90
Figure 6.2: The maximum effective sensing area of the IROD and IRDD simulated in SolidWorks	94
Figure 6.3: Experiment on can subjected to different loads.	97
Figure 6.4: Force Experiment on Pen Subjected to Different Load	97
Figure 6.5: The deformation of different egg in (a) and (b) subjected to different load.	98
Figure 6.6: The sensing sensitivity using 10k ohm as RM values on the actual Force Sensing Resistor from data sheet (Adopted from Interlinks Electronics, 2011)	99
Figure 6.7: The experimented sensing range of FSRs which the sensing area have been attached with rubber pad	100

Figure 6.8: Average force response corresponding to voltage output which is relative to load applied	100
Figure 6.9: Force response on FSR when grasping a can	101
Figure 7.1: The mickey mouse hole drilled at the pocket holes	104
Figure 7.2: The new location of the bearing	104
Figure 7.3: The new bearing housing location view in 3 Dimension.	104
Figure 7.4: The bearing is pushed out with ease using a screw driver via base.	105
Figure 7.5: The CSK screw hole that support the servomotor with finger body	106
Figure 7.6: Two 'U' shape palm with different labelling	106
Figure 7.7: The thin rod dowel pin on the left side and the dowel pin with angle on right side	107
Figure 7.8: Infrared Distance Detector's voltage output relative to distance sensing.	108
Figure 7.9: The L-shape fix at the side of the gripper's finger	109
Figure 7.10: The force sensors are attached at the middle of the finger body.	110
Figure 7.11: The force sensors are blocked by the joint	110
Figure 7.12: The reflective point of the IRDD at 4cm from the base and new reflective point at 1.5cm from the base by offset the IRDD into gripper.	111
Figure 7.13: The IRDD offset 35mm into the palm body	112
Figure 7.14: (a) The straight pad stacked at the finger tip. (b) Top view which shows the pad is in triangle shape.	112
Figure 8.1: The force sensors stacked in two rows	114

LIST OF SYMBOLS / ABBREVIATIONS

mm	millimetre, mm
m	meter, m
F	force, N
P	pressure, Pa
A	area, m^2
θ	<i>angle</i>
v	specific volume, m^3
V	voltage, V
M	moment of force, Nm
τ	torque, Nm
α	angle of twist
θ	<i>angle</i>
d_i	distance between Z_i and Z_{i+1}
C_i	cosine, $\cos\theta_i$
S_i	sine, $\sin\theta_i$
B_i	virtual link
IVOARM	In-Vitro Optical Aided Robotic Manipulation
BOM	Build of Material
IRDD	Infrared distance detector
IROD	Infrared object detector
IPE	IPE Automation Sdn. Bhd
PCB	Printed Circuit Board
RTC	Real Time Clock

LIST OF APPENDICES

APPENDIX	TITLE	PAGE
	APPENDIX A: The CAD drawing parts.	118

CHAPTER 1

INTRODUCTION

1.1 Background

Most of the industrial robot today employs unique method to grab and grip the object with the specific gripper, depending on the requirement. Most of them have actively employed the vision image to aid the gripping process. These give the information such as size, location, object type and others to the gripper. However, not all situations can employ the usage of machine vision. The following describe the challenges faced by the machine vision in industries.

The main component used by NASA for the assembly of the International Space Station is the space machine vision. Video camera based system, are attractive because of their ease of use, low maintenance and simplicity of integration to existing equipment (Blais, 2001). However, not all the machine vision can be employed to supervise the gripper. Presence of sun and other strong source of light adversely affect the quality of the conventional methods that rely on standard video images such as the camera on board the Space Shuttle. This has given poor disadvantage to the machine vision where light reflection on the surface of the components or material captured in the video will gives poor view to the engineer when assembling because the engineer need to uses the gripper to move the grip the material and component at exact location. Any wrong grip or collision will delay the time and damage the component as well as incurring high cost.

The Northern Digital Incorporate (Northern Digital Industry, 2010), a company specialize in medical field has stated in their website that “Although machine vision looks appealing from the perspective of minimal impact (with the exception of line-of-sight), there are many difficult implementation and environmental problems. These problems prevent machine vision from being broadly applicable. It is rare to find a machine vision solution that considers usability and minimizes application interference.” The interferences that stated by the Northern Digital Incorporate are the weakness of the machine vision such as line of sight between tracker and target, A less intrusive system typically means a less robust or flexible system, lighting conditions and background interference (complexity) can cause tracking problems.

1.2 Aims and Objectives

The aim of this research is to develop a gripper known as Design of In-Vitro Optically Aided Robotic Manipulator (IVOARM) and a new method which can perform ‘blind grasping’ without the aid of the machine vision and expected to achieve the following objectives:

1. Mechanical Design

Design a mechanical gripper which can host multiple sensors. The finger must be flexible in terms of number of degree of freedom and its angle of rotation must be independent from others. Determine the finger’s maximum force.

2. Sensors Development

a. Infrared Sensors Development

- i. Determine the best location for the Infrared Sensors.
- ii. Determine the angle of turning of the gripper’s finger relative to the infra-sensors.

b. Force Sensor Development

- i. Determine the limit of applied force on the specimen.
- ii. Determine the sensitivity of the force sensor used.
- iii. Determine the force respond of the force sensors attached to the gripper.

CHAPTER 2

LITERATURE REVIEW

Locating and determining the distance of the object from the gripper and using the proper way to grip the object is a major challenge to the industries which operates in variable environment such as space, medical field and others as mentioned in Chapter 1. Machine vision has proven to solve such problems by capturing the image of the object and calculating its distance from the gripper as well as the size of the object to let the gripper to use an appropriate way to grip on it.

However, there are several drawbacks on the machine vision system where its distance estimation and its disturbance of other source of light intensity as well as proper angle of viewing are the main concerns. In machine vision, distance determination is done by extracting the size of the object at its location relative to the camera position. This might create error if there is disturbance and lack of resolution. The light intensity of other source such as the sun which is strong enough will create the disturbance or noise during image capturing in space, as mentioned in Chapter 1. The angle of viewing of the camera and also its viewing path must be clear and no blocking is required so that image capturing can be done.

Force of the gripper's actuator onto object's surface is also considered a major concern where appropriate force will enable the gripper to lift up the objects. Last generation of robotic arms are lacked of force sensors. Excessive force being employed will damage the objects or leave the gripping mark on the objects surface (Xu DeZhang, et al, 2005). Proper force should be applied with the use of strain gauge sensors to obtain ensure there is no excessive force.

Many studies have been performed on the method to locate, size determination and grasp the objects. Notable research such as **“Robot Grasping of Unknown objects (Redwan Alqasemi, et al, 2007), Development of the robot gripper for a Home Service Robot; Design and Construction of a Robotic Gripper for Activities of Daily Living for People with Disabilities (Christophe Leroux, et al, September 2007), High Performance Robotic Gripper Based on Choice of Feedback Variables (Zaki, A.M. ,et al, 2010)”** have been referred to overcome the problem

2.1 **Robot Grasping of Unknown objects, Description and Validation of the Function with Quadriplegic People**

Robot Grasping of Unknown objects, Description and Validation of the Function with Quadriplegic People (Christophe Leroux, et al, September 2007) employs the tactics of using machine vision attached to the gripper to detect the distance of the object relative to the video camera. On the gripper, stereoscopic video cameras are attached on it. These camera will capture the image and send to the user by displaying the real time image on the screen. The operator will then control the gripper with the body part which is still functioning well such as hand or leg. There are three phase for this gripping method. Using the only information which is being displayed on the screen, the operator try to control the movement of the arm to adjust the location of the gripper close to the object target. This corresponds to the designation phase. After he or she has determine the object to be grip, the gripper will approach the object via robot arm movement, with the 2-D real time displayed on the screen. This corresponds to the approaching phase. Once the gripper is in position, gripping is triggered and the object is brought back near the operator which is the final phase.

2.1.1 Flow chart

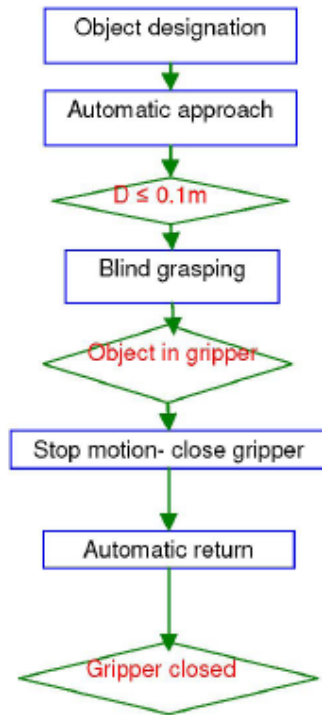


Figure 2.1: The flow chart on the MADEUS operation (Adopted from Christophe Leroux, et al, 2007)

The flow chart in the figure 2.1 shows the MADEUS gripper operation in details. The object in the screen is selected by the users. Once the object is determined, the arm will automatically approach to the object, with the aid of the stereoscopic video camera. When the object is within the 0.1m in the gripper, the gripper will proceed with blind grasping without considering the object actual position in gripper. Once the gripper has grip, the motor will stop to hold on the position. Then, the arm will retract and bring the object back to the user. Once the object is retrieved, the gripper will close to protect its mechanism.

2.1.2 Distance Estimation

The distance estimation of the object relative to the video camera is obtained by extracting the size of the object in the image captured by the video camera. Based on the size of the object in the video camera, the arm will move the gripper to the object using the estimated distance value from the system.

2.1.3 Feature extraction

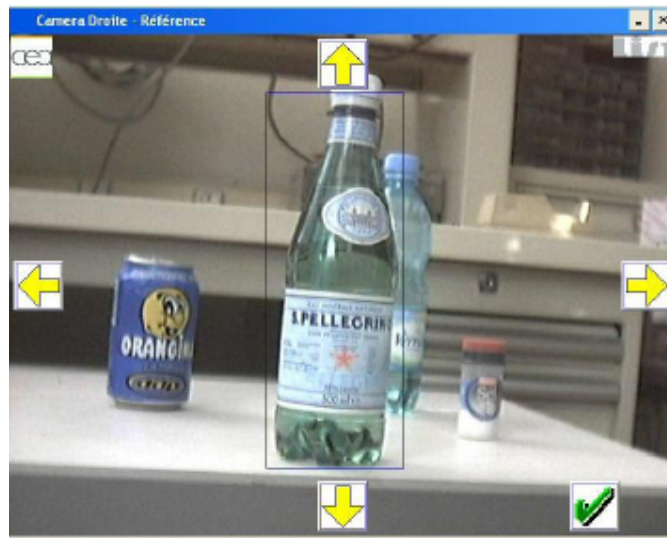


Figure 2.2: The flow chart on the MADEUS operation (Adopted from Christophe Leroux, et al, 2007)

A image of area will be selected by the user via the focusing program. Once the area in the image defined, it is necessary to locate and "identify" the object truly indicated by the operator. The location is determined by estimate the size and resolution of the object which in turn dominate the whole image. The method uses to select the correct object to be grasped is the 4 buttons in the image. If the first location of the object desired is wrongly indentified by the system, the users will click on one of the button to shift the box concentration on other objects defined in the image for the system correction. For this stage, interest points are computed using Harris and Stephens feature detector.

2.1.4 Matching and localization

When extracting the features, the selected objected on the screen have to be matched with the actual object for the arm identification. The matching process started with the point to characteristic point matching.

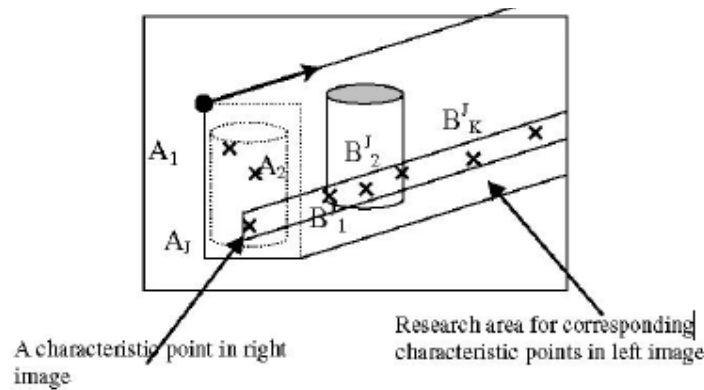


Figure 2.3: The matching and localization (Adopted from Christophe Leroux, et al, 2007)

The process (Christophe Leroux, 2007) in this system is explained as following:

1. For each feature point A of image I , we look for feature points B of image I_r which satisfy the epipolar constraint with a given error as shown in figure 2.3.
2. Eventually some points B_r^I are eliminated with a i_k correlation measure. Selection using this measure is very weak (high threshold adjusted among experiences) and very small time consuming. This stage is not fundamental but it can improve the statistical matching performances in "limit" cases: when there are few corner points or a great number of corner points.
3. For each point B_r^I we compute the i_k displacement $A_I = A(A_i, B^I)$ expressed in pixels with respect to point A_f . In our case $A(A_I, B^I)$ is simply the Euclidian distance between the two pixels along the epipolar line.
4. We then look for the most frequent value A_m for the A .
5. We then define the matching point for A_I as being the point B having the closest A_I value to A_m in a predefined limit. If no A is found within this limit, we consider that point A_f of freque image I , does not have any correspondent in image ' r '

Once all the matching assumptions carried out, the selection of the object consists in retaining the most frequent distance computed. This distance is corresponded to the indicated object. Using the barycentre of the matching points, the direction of the object is located and the distance is estimated.

2.1.5 Evaluation

The gripper Madues relies heavily on machine vision system to identify and calculate the distance which is all in approximation based on the image obtained. If the image is distorted by noise at the moment of calculation, the calculation will have big error. The robot arm have to repeating to approach the objects on several time before able to determine the exact location to confirm the estimated value.

2.2 High Performance Robotic Gripper Based on Choice of Feedback Variables

The High Performance Robotic Gripper Based (HPRG) on Choice of Feedback Variables (Zaki, A.M. ,et al, 2010) uses the simple mechanical design with 2 fingers parallel design without considering its flexibility. One of the finger is fixed and the other is movable and both shape is rectangular shape as shown in figure 2.2.4 The movable finger is derieved on a lead screw and guided by a linear bearing system. It is has self locking capability by stoping the lead screw from turning. The sensors being employed in this gripper are Flexiforce A201 to detect the force applied and Phidget vibrator sensor to be used to detect slip. Permanent magnet BLDC brushless dc motor is used in this gripper due to its low rotor inertia.

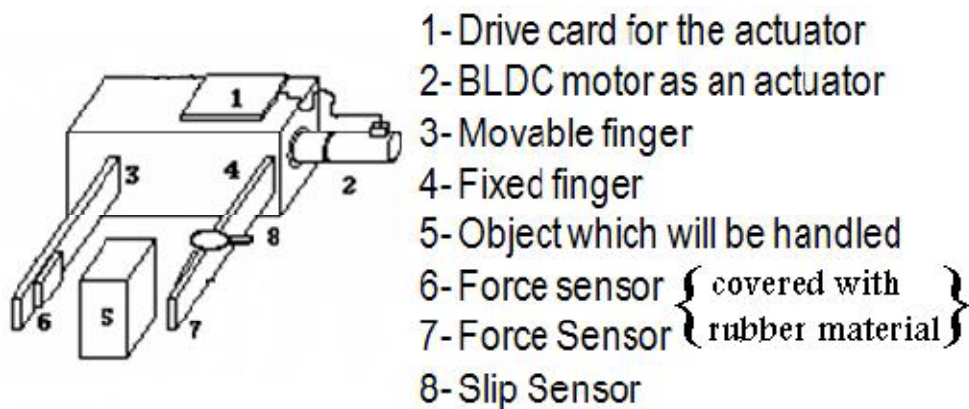


Figure 2.2.4: The mechanical design of the HPRG gripper (adopted from Christophe Leroux, et al, 2007)

2.2.1 Mechanical design

The mechanical design of the HPRG is simple to demonstrate the effectiveness of the sensors attached to its finger. Two flat plate fingers are used and the length of these two plate is 15 cm which requires high develop torque from the dc motor. The width of these plates are fit to size of the sensors attached on it. The movement of the gripper is control by the lead screw, by rotating the proper direction will open or close the gripper.

2.2.2 Sensors

2.2.2.1 Force sensors.

The force sensor being employed is A201 which is used to detect only force employed on it. The force sensors are covered with rubber to increase the friction coefficient μ so the object gripped will be sticking on the rubber surface. Voltage generated from the force sensor will be used to measure the force applied onto the finger.

2.2.2.2 Slip sensor

The slip sensor being used is the Phidget vibrator sensor which is used to detect the vibration on the gripper. Since the object is in steady position in the gripped position, any external force will tends to break this steady state. Once the external force is applied, the vibrator will detect the vibration of the gripper and the object might slip away from the gripper finger. Then, the gripper will apply more force onto the object to ensure the object do not fall out.

2.2.3 Evaluation

The design of the gripper is simple and matching with its objective. However, the finger designed is lacking of flexibility with detecting the force only on two points. There is high chance of rotation motion occurred on the object while gripping.

2.3 Design and Construction of a Robotic Gripper for Activities of Daily Living for People with Disabilities

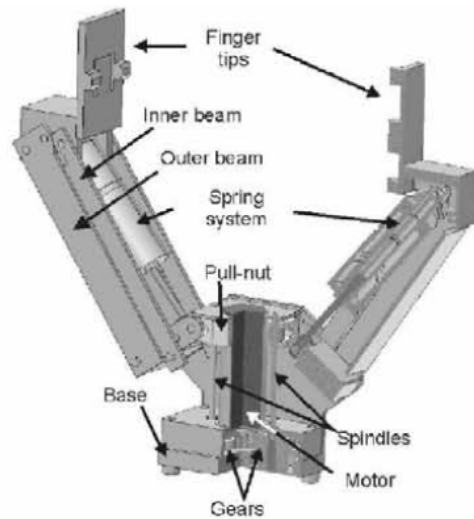


Figure 2.5: Manus gripper internal mechanical part (adopted from Redwan Alqasemi, et al, 2007)

Design and Construction of a Robotic Gripper for Activities of Daily Living for People with Disabilities (Redwan Alqasemi, et al, 2007) uses the Manus gripper which consist 2 fingers gripper to grip the object. The purpose of building this gripper is serving the disabled person at home. This gripper fully employs mechanical components to enforce gripping performance and controled using one motor.

The fingers' tip can be changed to suit the daily activities of the disabled. Using the lead screw, the motion of close and open can be controlled by attaching the screw to the motor and the motor spins. The gripping operation is depending on the machine vision system, which controlled directly from user's sight.

2.3.1 Mechanical Design

2.3.1.1 Mechanical Movement

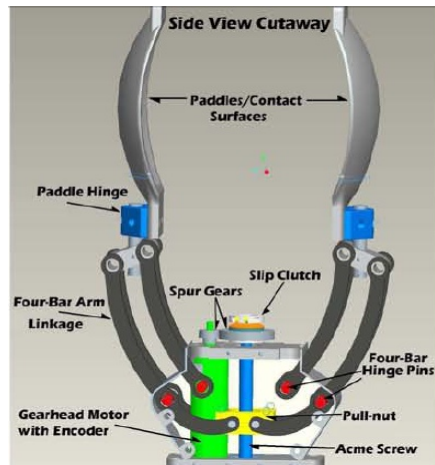


Figure 2.6: Manus gripper internal mechanical part (adopted from Redwan Alqasemi, et al, 2007)

The Manus gripper movement in figure 2.6 is summarized below:

- I. The motor turns the gears which turns the acme screw.
- II. The acme screw will be turned and move the pull-nut which turns the four bars hinge pins.
- III. The spur gear is turned in the same time as the acme screw turn to open up the fingers.
- IV. The spring will be pulled which put the gripper fingers in tension form and grip the objects.
- V. When the motor turn in different direction, the acme screw will turn in opposite way to make all the components back to initial state.

2.3.1.2 Design of the Fingers' Tip

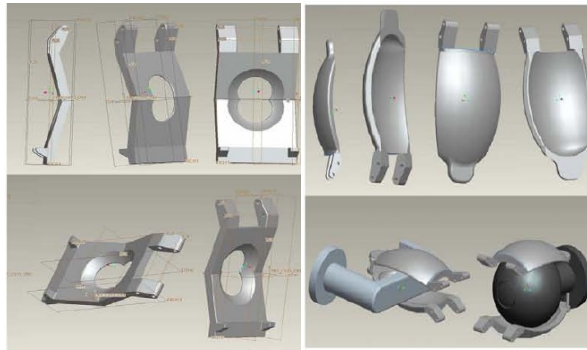


Figure 2.7: Various finger tip of the Manus Gripper (adopted from Redwan Alqasemi, et al, 2007)

The finger tip in this gripper is designed to be universal, which means the finger tip can be in any shape. The purpose of making it universal is due to under different circumstances, the finger tip can be changed to achieve the objective.

2.3.1.3 Evaluation

The Manus gripper is a good design which fully utilize the mechanical structure. However, its flexibility is not so high because the gripper's finger has one rotation motion. The surface of the finger cannot be attached with any force sensors due to lack of space. The force of gripping can only be estimated via the machine vision system it has stated early. Each angle of finger's joint is not controlled independently. One motor's movement will define the all angle of the joint.

Table 1: Evaluation on each of the grippers with IVOARM

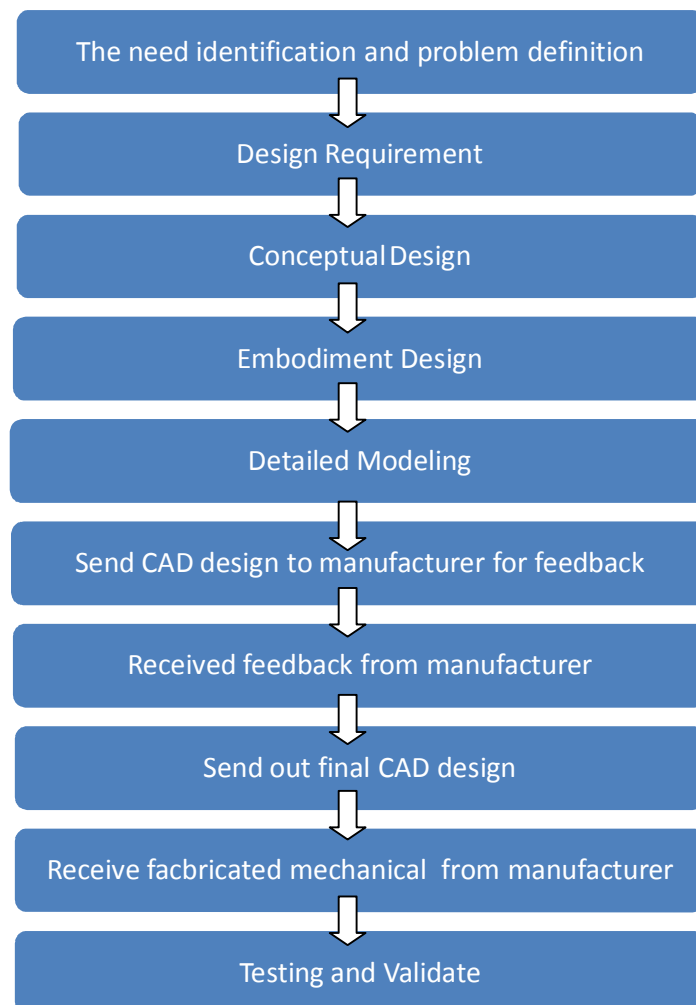
	Flexibility	Degree of freedom	Gripping envelope	Area of surface contact on circle object	Sensors attached	Driving mechanism	Joints on each link is controlled independent?
MADEUS	2 parallel link with 2 joint	2	medium	High	Force sensors	lead screw and gear drives all screw	No, each joint angle is relative to the first one which drives by lead screw
Manus	2 link finger with 2 joint	4	low	Medium	Force sensors and infra red sensor	One lead screw drives all joint	No, each joint angle is relative to the first one which drives by lead screw
HPRG	2 parralle link	none	low	Very low with two contact point	Force sensor and vibration sensor	lead screw in one direction	No. Do not have joint angle.
IVOARM	one has 3 link finger with 3 joint and one has 2 link finger with 2 joint.	5	High	High	Force sensors and infra red sensor	servomotors on each joint	Yes, the servomotor on each joint can be altered independently from others.

CHAPTER 3

METHODOLOGY

3.1 Project Design Overview

The primary concern of this project is the mechanical design procedure and sensors development for the prototype. The workflow is shown in figure 3.1 and figure 3.2.



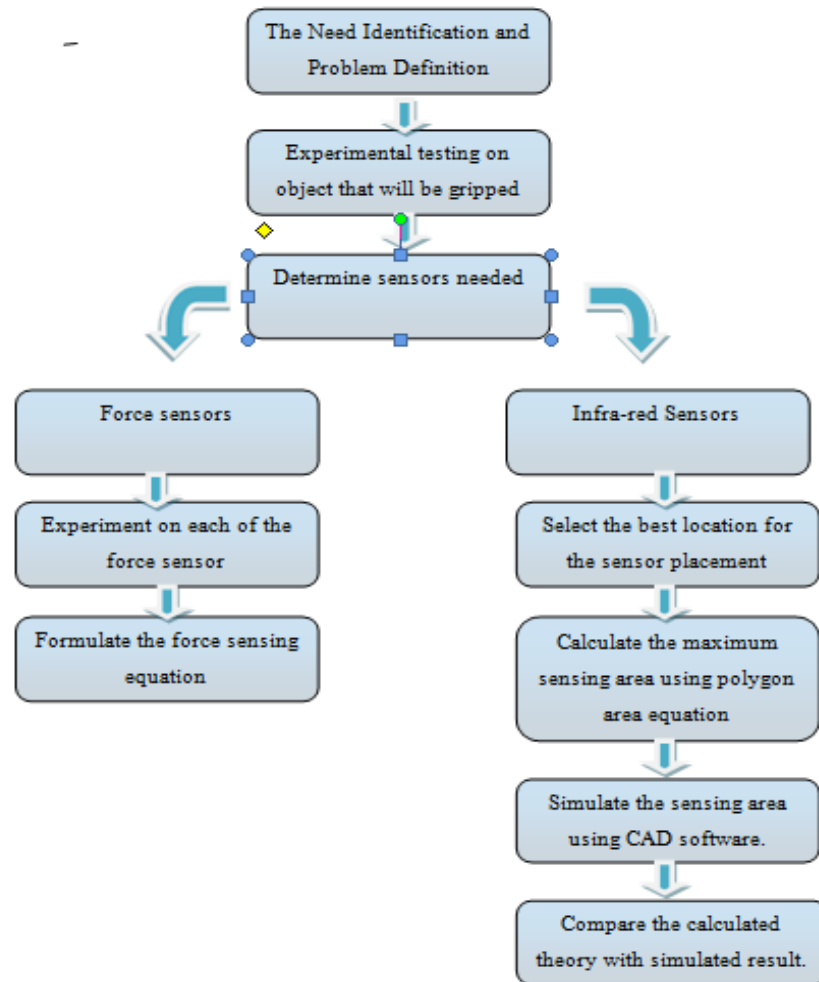


Figure 3.2: Flowchart sensor development

3.2 The system

After a Literature review is done in the Chapter 2 to gather some information and generate idea before planning the experiment layout. The overall system is named In-Vitro Optically Aided Robotic Manipulation (IVOARM). It has contained three sub systems: mechanical parts, electronics system and algorithm development.

In mechanical parts section, it can separate into two components: Robotic Manipulator and Foundation Settlement. Robotic Manipulator is the main body of IVOARM, which is mechanical structure to perform object's detection and grasping object. Foundation Settlement is a fixture stand used to holding the robotic manipulator in static environment. This mechanical design will be divided into sub components for further experiment.

In electronic system, it will be divided into two parts, which is circuit and sensors. The circuit and sensors part will be focused on experiment their characteristic. In algorithm development, this part will be focused on developing equation and implement suitable programming part to move the gripper. The electronic part and algorithm part will be handled to another team member, Mr. Cheng Chia Loon.

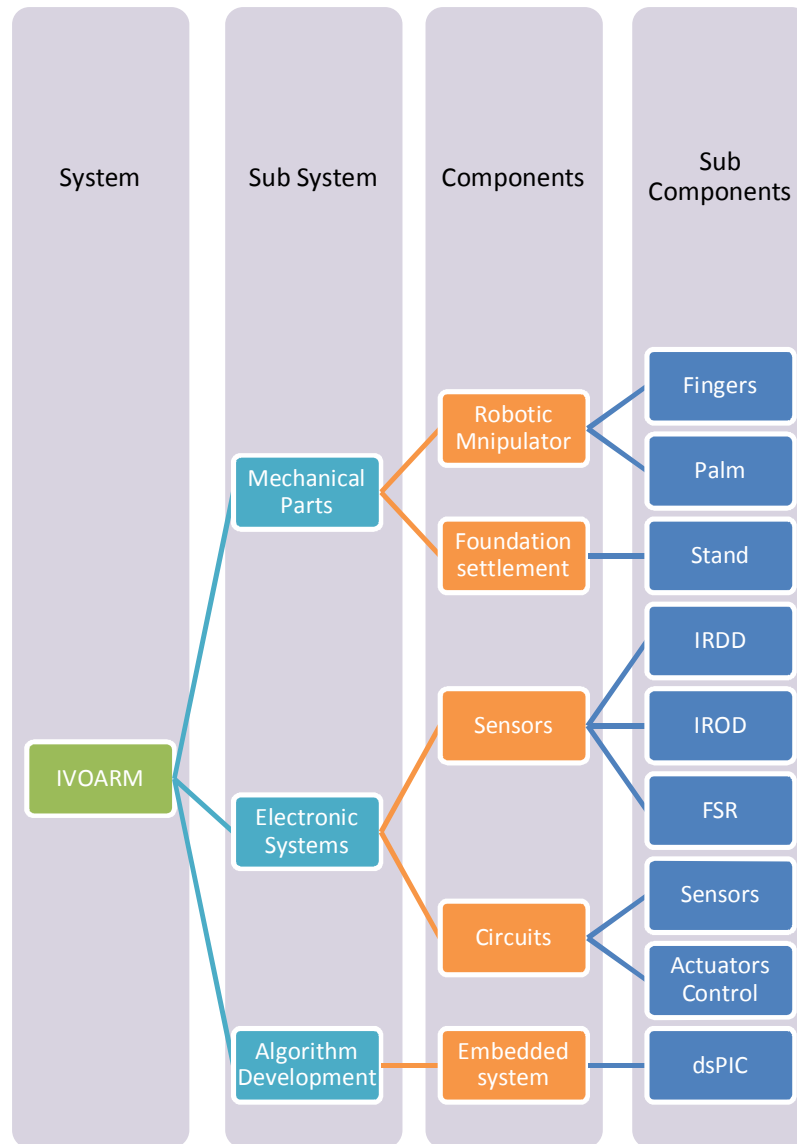


Figure 3.3: IVOARM whole system

3.3 Project Management

Project management is drafted before the further actions are taken. In this project, planning acts an important role, it might lead project to neither success nor failure. This project has lead by the four management functions: Planning, Organising, Leading and Controlling (POLC) have stated in figure 3.3:



Figure 3.3: POLC process flow

According to New Era of Management (Richard L. Daft, 2008), Planning means identify goals and deciding tasks and use of resources needed to attain them. In planning stage,

Organising typically follow planning and way to accomplish the plan. Organising involves assigning tasks, grouping tasks, allocating resources for tasks. Examples like Gantt chart, design procedure for each sub systems, allocating resources and tasks scheduling. This project has involves mechanical parts, electronics circuit and algorithm development. Hence author has separated tasks respect to ability of team members and assigning tasks details to each of them.

Leading is the use of influence to motivate team members to achieving goals. A good leader must able to create a shared cultures and values, communicating goals and influence employees to perform at higher level.

Finally is Controlling, controlling is fourth function in the management process. It means monitoring team members activities, determining whether the project team is on target toward its goals, and make correction as necessary. Example is every two weeks our Project Supervisor will give guidance and coaching to ensure the project keep on track.

3.3.1 Gantt chart

The Gantt chart is planned to ensure all the sequences of the project are done on time. Appropriate assignment of time on each of the sequence is done by making it into Gantt chart management as shown in Appendix A. Literature review will use up to four days for analysis. The mechanical design of IVOARM will be plan first. The mechanical design will use up to 23 days to ensure the parts are able to be fabricated out. These 23 days includes the purchase of suitable electronic components to be used and this will takes around 1 week to gather all the components. The circuit design is then implemented to suit the usage of electronic components which drive the mechanical part.

Once the mechanical part is assembled, it is tested run with simple mechanical movement to ensure its reliability. Next, the algorithm is formulated to ensure the initial objective can be achieved in programming part. This formulation will take up to 4 days. The algorithm is then programmed into the electronic embedded system to test run the mechanical part. Additional time has been reserved to fine tune the program.

When the program is done, experiment will be done to ensure the objectives which are stated in aim and objectives in 1.2 will be achieved. The final step is the thesis preparation which compiles the whole project sequence. This project estimates to be completed within 44 days.

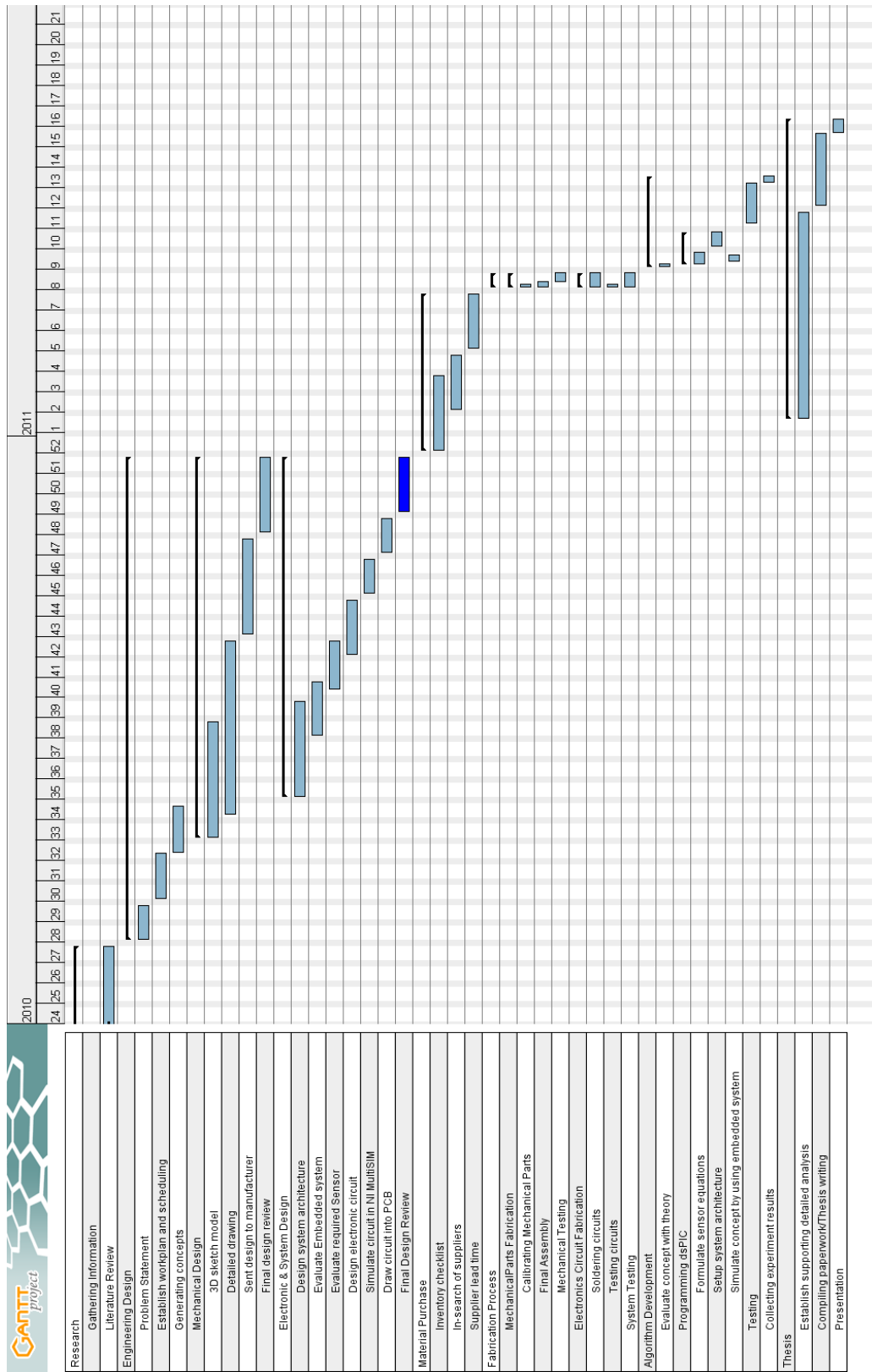


Figure 3.4: Project Gantt chart, colour indicate time to planned schedule to complete the tasks and black line indicates total period to complete a sub system

3.4 List of Tools

After completion of Root Cause Analysis, the project has stated from concept design into detail design, after discussion among team members, the author has listed all required tools into two sections, hardware's and software's.

3.4.1 List of hardware

Table 2: List of hardware

Items Used	Description
Mechanical tools	Screw drivers, spring, saw and L-shape ruler.
Sensor parts	Force Sensing Resistor (FSR), Infrared Distance Detector (IRDD) and Infrared Object Detector (IROD)
Software	Microsoft Excel and SolidWorks

Due to the limitation of funding, allocating resources are important. Some the tools required can borrow or requested from Universiti Tunku Abdul Rahman's (UTAR) workshop. This can reduce the unnecessary expenses and save fund for other purpose.

In this project, some of the equipment are loan or utilised from different places, like Agilent Technologies has loan a Precision Measurement Equipments to this project. Some equipment can be requested and use in workshop, like drilling machine and INSTRON 5582 for experiment on force testing.

3.4.2 Virtual Mechanical Design in SolidWorks

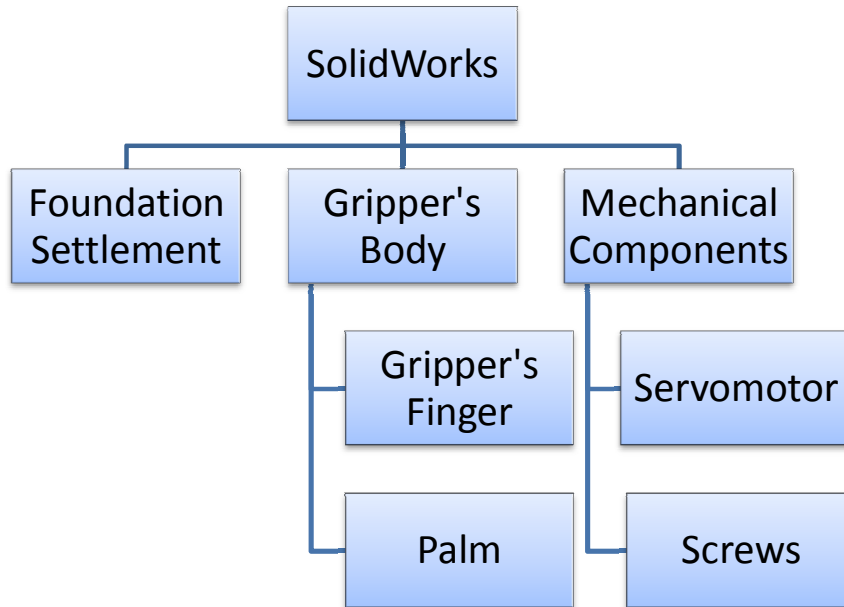


Figure 3.5: List of virtual designs drawn in SolidWorks

The IVOARM gripper will be design in SolidWorks. The figure 3.5 shows the part that will be designed in virtual form before sending out for fabrication.

CHAPTER 4

MECHANICAL DESIGN

4.1 Engineering Design

The engineering design of the IVOARM gripper is listed in a flow chart as shown in the figure 3.1. The figure 3.1 shows the overview of the design process which involves the specific task and steps needed to complete the design process. The engineering design process starts with the need of identification and problem definition. It will then focus on the design requirement on the gripper that will be design at the conceptual level. Base on the design requirement, the conceptual design will design a rough model which fulfils the requirement.

After conceptual analysis, the embodiment design will start based on selected conceptual design. The completed design will be created into CAD drawing and send to the manufacturer to fabricate. Once the parts are received from fabrication, checking and validation is done to ensure no dimension is wrong or missing parts.

Once checking is done, the parts will be assembled in steps as shown in figure 3.2. The assembly of the parts will consist of components that are available in the inventory. If the components needed are missing, purchase has to be made. If the parts are not available in the market, it must be fabricated by the manufacturer. Once all the parts are gathered, the assembly of all the parts can be completed. The characteristic of the gripper such as force that can be sustained will be tested.

4.1.1 **The need identification and problem definition**

As mentioned in introduction, the gripper will perform 'blind search' to grip object. 'Blind search' is a method to search an object without the presence of the machine vision and depends on the aid of the non-visual sensors. In order to perform 'blind search', the gripper needs to have 'guidance' which is the sensors. The sensors location on the gripper will determine the sensing area which the 'blind search' can be executed.

4.1.2 **Design Requirement**

As analyzed in Table 3, the gripper is required to have following characteristic:

1. Can grasp can, egg or tin in open loop.
2. Surface of the finger must be wide and able to host sensors on it.
3. The sensors are in the location that is able to detect the object within the grasping range.

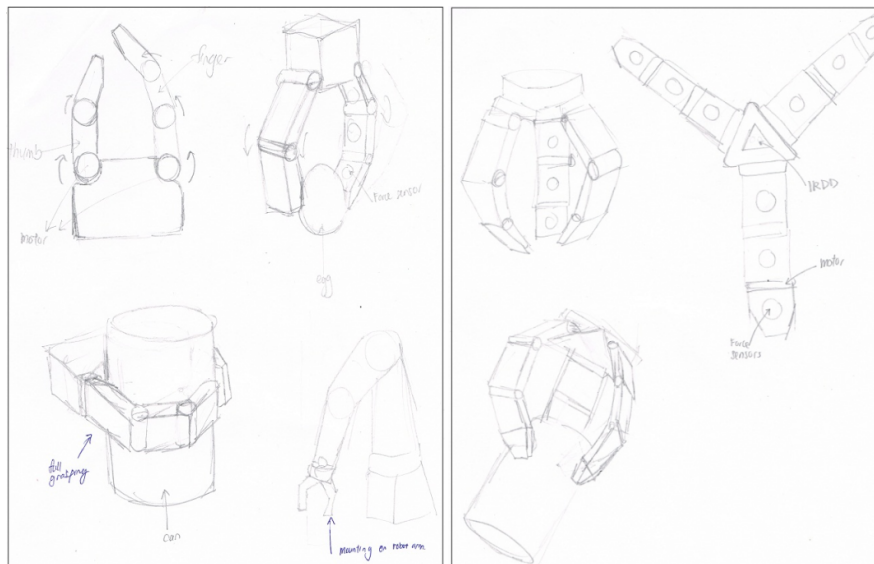
Once the entire requirement is determined, the next stage will be conceptual design in which the best and economical design will be chosen.

4.1.3 **Conceptual Design**

Before designing the mechanical structure, conceptual design on grippers are needed to be looked into. The conceptual design of the gripper will be sketched on a paper to be analyzed before the selection can be made. Figure 4.1 shows the various conceptual designs on the sketch papers.

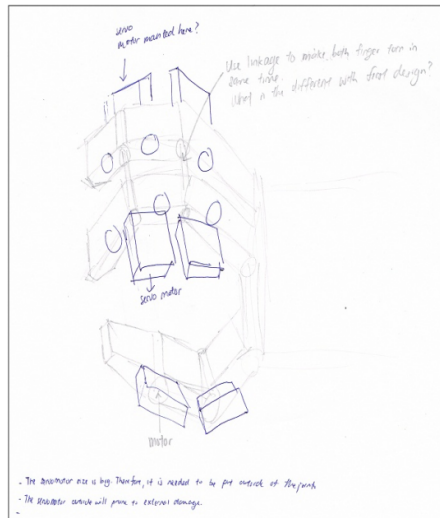
Table 3: Comparison of conceptual designs

Design	A	B	C
Number of finger	3	3	3
Joint's degree of freedom	5	9	8
Number of joint	5	9	8
Cost to manufacture	Medium	High	High
Structure Complexity	Low	High	High
Finger contact with object's surface	High if using full grasping	Low due to octopus gripping	High if using full grasping
Gripping envelope	High if using full grasping	Low due to octopus gripping method	High if using full grasping
Gripping stability	at full gripping envelope and finger tip	Yes, at full grip and finger tip	Yes, at full grip and finger tip
Proposed Servomotor position	In the gripper's finger body	Outside the gripper's finger body	Outside the gripper's finger body



Conceptual A

Conceptual B



Conceptual C

Figure 4.1: Comparison of various conceptual designs.

The conceptual design A consists of two finger gripper with five joints. The number of degree of freedom is same as its joint. The cost of manufacturing is lower than the others due to its small quantity of component parts. The gripping stability can be achieved at the finger tip but the rotational moment can cause the slip which must be addressed. On full grip, the object can be stably gripped without the effect of rotational moment. However, it can be addressed by adding three stacking horizontal and parallel plate at the finger tip to address this issue. The structure complexity is low comparing the others and its maximum contact with object's surface is high in full grasping. The servomotor can be inserted into body of the finger.

The second design is consisting three fingers with three joint on each. It is the most complex among the conceptual design. Their numbers of degree of freedom are same as its number of joint. Its cost of manufacturing is the highest among the others and its structure complexity is high. It has the most stable in terms gripping. However, the maximum envelope of gripping is the lowest among the others. The servomotor at the joint is needed to be placed outside the finger body due to the space conservation. The servomotor positioned outside the body might prone to external damage.

The third design is a three finger gripper which two of the finger is parallel on the right side and consist of one finger on the left side. The numbers of degree of freedom are same as its number of joints. Its cost of manufacturing is high because its number of components needed to be manufactured is high. The maximum gripping envelope is high and its gripping in terms of stability is high. However, during the finger tip gripping, both of the gripper fingers on the right side must have same vector and degree. This is due to the fact that the joints are controlled by independent servomotors. Any mismatch between the joints' servomotors between two fingers will cause the object at finger tip to drop.

After studying on the proposed conceptual designed, two finger grippers with anthropomorphic motion are chosen since it is lower cost and least complex compares the others. Furthermore, the servomotor is put in the body of the gripper's finger which serves as the protection. Its gripping envelope and its object's surface of contact is high too.

4.1.4 **Concept Theory**

Next, the information on the specific theory is focused on. The specific theory mentioned is related to the design process of the gripper. Some of the important theories are specified below:

1. Kinematic of gripper
2. Polygon Area

4.1.4.1 **Kinematic of gripper**

Kinematic of gripper is the main focus on this project as it will determine the whole structure's movement. Since the length of the gripper will be determined manually and the angle of each joint is variable, the kinematic used in this project will be forward kinematic as it can determine the position of each linkage.

4.1.4.1.1 The forward kinematic

Based on the designed, the forward kinematic is shown in figure 4.2.

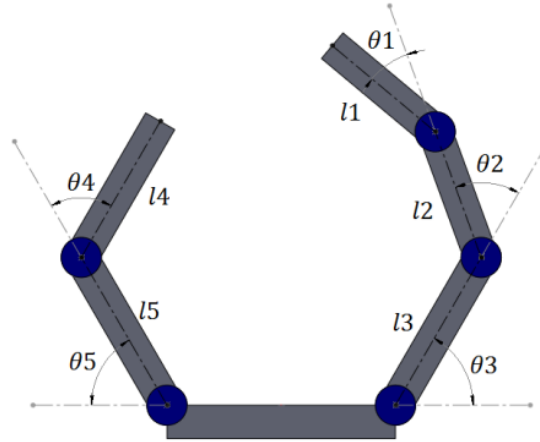


Figure 4.2: Kinematic of gripper

For the right finger gripper,

$$T1(\theta1) = \begin{bmatrix} \cos(\theta1) & -\sin(\theta1) & 0 \\ \sin(\theta1) & \cos(\theta1) & 0 \\ 0 & 0 & 1 \end{bmatrix} \quad (1)$$

$$T2(\theta2) = \begin{bmatrix} \cos(\theta2) & -\sin(\theta2) & l1 \\ \sin(\theta2) & \cos(\theta2) & 0 \\ 0 & 0 & 1 \end{bmatrix} \quad (2)$$

$$T3(\theta3) = \begin{bmatrix} \cos(\theta3) & -\sin(\theta3) & l2 \\ \sin(\theta3) & \cos(\theta3) & 0 \\ 0 & 0 & 1 \end{bmatrix} \quad (3)$$

$$T4 = \begin{bmatrix} 1 & 0 & l3 \\ 0 & 1 & 0 \\ 0 & 0 & 1 \end{bmatrix} \quad (4)$$

$${}^e_e T = {}^4_0 T(\theta1 \ \theta2 \ \theta3) \quad (5)$$

Where ee is end effector and the b is the base.

Then,

$$\begin{bmatrix} x \\ y \\ 0 \end{bmatrix} = T \begin{bmatrix} 0 \\ 0 \\ 1 \end{bmatrix} \quad (6)$$

Thus, the forward kinematic complete equation is

$$x1 = l_3 \cos\theta3 + l_2 \cos(\theta2 + \theta3) + l_1 \cos(\theta1 + \theta2 + \theta3) \quad (7)$$

$$y1 = l_3 \sin\theta3 + l_2 \sin(\theta2 + \theta3) + l_1 \sin(\theta1 + \theta2 + \theta3) \quad (8)$$

For the left finger gripper,

$$x4 = l_4 \cos\theta4 + l_5 \cos(\theta4 + \theta5) \quad (9)$$

$$y4 = l_4 \sin\theta4 + l_5 \sin(\theta4 + \theta5) \quad (10)$$

4.1.4.2 Polygon Area

The polygon area is a measurement of an area which is enclosed by the linear boundary which is linked between three points or more. The position of the infrared sensors can affect the maximum area of sensing. Infrared sensors' position can be determined by calculating their sensing area within the gripper using the polygon area formula. Since the Cartesian coordination is used on each finger position, the Beyer formula can be used to calculate the area. The figure 4.3 shows the principal of Beyer formula.

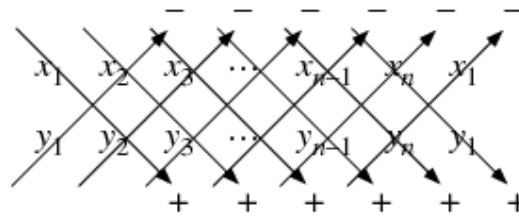


Figure 4.3: Non-self intersecting planar to calculate determinant. (Adopted from Eric Weisstein, 2011)

The (signed) area of a planar non-self-intersecting polygon with vertices (X_1, Y_1) , ..., (X_n, Y_n) is

$$A = \frac{1}{2} \left(\begin{vmatrix} X_1 & Y_2 \\ Y_1 & Y_2 \end{vmatrix} + \begin{vmatrix} X_2 & Y_3 \\ Y_2 & Y_3 \end{vmatrix} + \dots + \begin{vmatrix} X_n & X_{n-1} \\ Y_n & Y_{n-1} \end{vmatrix} \begin{vmatrix} X_{n-1} & X_1 \\ X_{n-1} & Y_1 \end{vmatrix} \right) \quad (11)$$

Where ,

A = area

$|M|$ = determinant

4.1.5 Embodiment Design

The embodiment design in this project will focus on the desired requirements and the ease of assembling and disassembling on each part. The assembling and disassembling process is important as the gripper components might needed to be changed or replace with others. High complexity design will hinder the ease of assembling and disassembling process. This will make the components replacement to be more difficult.

4.1.5.1 Component Selection

Some of the parts in the gripper are not designed and built manually. These parts will be purchased from the market and selection of the components will be crucial to the gripper's performance.

4.1.5.1.1 Infrared Red Object Detector

Function: The infra red object detector in the IVOARM will be used to detect the presence of the object approaching near the gripper finger surface.

The sensing range must be around 1cm to 3cm. Size of the IROD must be small enough to attach to the gripper's finger. Lastly the cost must be low. Table 4 is used to compare the TCRT 5000 and TCRT 1000. TCRT 5000 and TCRT 1000 has almost same characteristic due to its same family series. However, the TCRT5000 is chosen due to its high sensing range and its sensing range can be adjusted with limiting the current supplied to it. The price is an advantage and the TCRT1000 is an old type sensor which is hard to be found in market compares to TCRT 5000.

Table 4: Comparison of Infrared Object Detector TCRT family series

	TCRT5000	TCRT1000
Price	RM2.50	RM3.06
Sensing Range	2.5cm	1 cm
Detector type	Phototransistor	Phototransistor
Size	10.2 x 5.8 x 7	7 x 4 x 2.5
Features	Daylight blocking filter	Daylight blocking filter
Output current	1 mA	0.5 mA

4.1.5.1.2 Motor

Function: The motor installed into the gripper finger will be used as a joint between links.

The motor must be light in weight. The positioning control of the motor must be precise. The torque of the motor must be reasonable in order to provide appropriate force. Besides that, it must handle high current input so the maximum force can be achieved without burning out the motor. Moreover, the cost must be low since the IVOARM requires a lot of servo motor to fit at the joints. Table 5 shows the comparison among the motor gathered from catalogues and internet. HS-56HB is chosen over the others due to the fact that it is light in weight which is around 10g and very precise with 1 degree per step. It consumes low power which is suitable to our board development later on. The price is fair given the advantageous it possesses compared to the others.

Table 5: Comparison of Motor

	MO-STEP-17PM-J3X	MO-SPG-30E-20K	HS-56HB
Type of motor	Stepper motor	DC Gear motor with encoder	RC servo motor
Size	large	large	small
Supply voltage	6~12v	12v	6v
Torque	7.9mNm	78.4mNm	1.4kgcm
Angle resolution	1.8 degree/step	1.5 degree/step	1 degree/
weight	250g	225g	10g
Precision control	high	medium	Very high
Cost	Rm50	Rm70	Rm68

4.1.5.1.3 Selection of distance detector

Function: The distance detector will be used to detect the presence of the object in the gripping area of the IVOARM.

The selection of distance detector for IVOARM must have reasonable range of detection. Since the object will be approached by the gripper, the near distance sensing must be considered. The sensor resolution must be high so that the conversion into voltage will be high. Moreover, the size must be small so that it can be fit into the IVOARM body and the cost must be low.

Table 6 shows the comparison between Ultrasonic Range Finder and the SHARP GP2D120. SHARP GP2D120 is chosen over Ultrasonic Range Finder due to the fact that the media used by the SHARP GP2D120 is infrared. The wavelength that emitted by Ultrasonic Range Finder will be deflected easily in the IVOARM. Ultrasonic sensor wave is easy to be reflected due to the reflection from different angle of the finger. For example, when the gripper's finger is closed, the internal surface of the gripper's fingers will reflect the wave and makes the distance measurement inaccurate. Thus, it has high interference. SHARP GP2D120 has a very fast refresh rate and its cost is much lower than Ultrasonic Range Finder.

Table 6: Comparison of Ultrasonic Range Finder and the SHARP GP2D120.

Specification	Ultrasonic Range Finder	SHARP GP2D120
Supply voltage	2.5v~5v	4.5~5.5v
Signal output	Analog or UART	Analog
Sensing distance	0~6.45m	4~0.4m
Size of sensor	medium	small
Sensor media	ultrasonic	Infrared
Interference	High	Moderate
Sensor refresh rate	50ms	36ms
Cost	Rm140	Rm60

Function: The force sensors in the IVOARM gripper will be used to measure the forces applied to the object.

Table 7 shows the characteristic of different sensors. The selected force sensor must be small in size, light in weight, high sensitivity in sensing which ranging from 100g and above and have reasonable sensor resolution. FSR Part-402 is chosen over the others due to its tactile sensor type which is small in size and thin in term of thickness. It also has the sensing range of 100g and above and come in various sizes. It also has reasonable sensor resolution and the cost is the lowest comparing to others.

Table 7 Comparison of Force Sensors' Characteristic

Specification	FSR Part-402	FS20	ENDEVCO Model 2312
Type of sensor	Tactile sensor	Low force compression	Piezoelectric Force Sensor
Force sensing range	100g~10kg	750g~1500g	0~7kg
size	various size	small	Small
Supply voltage	2~12v	3.3v~12v	5v~12v
Response time	fast	fast	fast
Sensor resolution	medium	high	high
Cost	Rm23	Rm45	Rm33

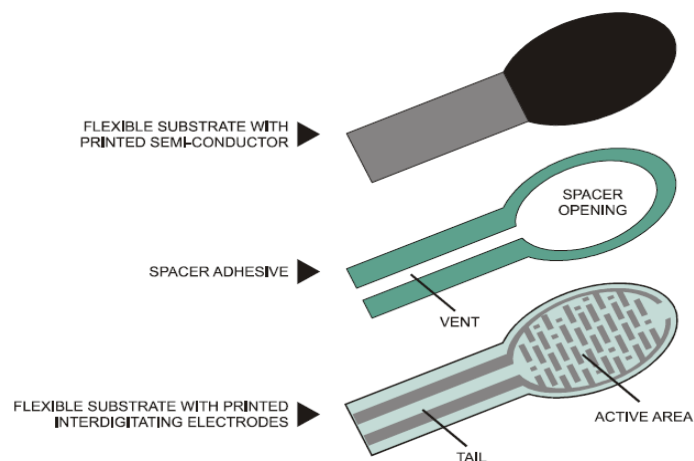


Figure 4.4: The layer structure of force sensors

(Adopted from Interlink Electronics, 2011)

4.1.5.1.5 Bearing

Function: Reduce the friction of the linkage rotation.

The ball bearing will be used in the IVOARM as the coupler to reinforce the strength of the motor joint. It is also used to eliminate the friction via the rolling of the ball bearing. Figure 4.5 shows the bearing used in the IVOARM.

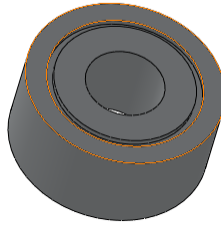


Figure 4.5 The bearing for the joint of IVOARM

4.1.5.1.6 Dowel Pin

Function: Dowel pin is used to maintain the connection between joints.

The dowel pin will be fixing at the bearing and the gripper finger joint. Its function is to connect the linkage between the gripper's finger bodies. It is also used to fix the gripper's joint linkages so the alignment of the finger's body will not run away. Figure 4.6 shows the dowel pin which is 1mm.

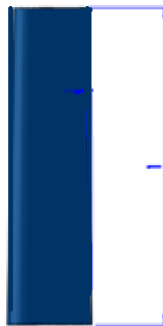


Figure 4.6: The dowel pin

4.1.5.1.7 Coupler

Function: The coupler will be used to connect the motor and the link as well as to maintain the connection between joint and drive the joint movement.

The coupler is provided by the servomotor's spare parts as shown in figure 4.7. The length of its side is long which it sustain high force to drive the rotation.

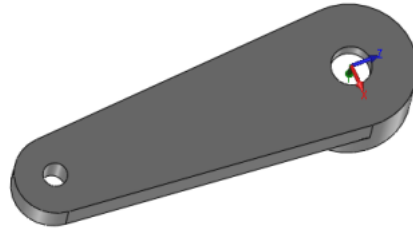


Figure 4.7: The motor coupler

4.1.5.1.8 SolidWorks

SolidWorks is a Computer Aided Design (CAD) software used to design and simulate the designed components to view their characteristics and their movements. SolidWorks has various functions such as length measurement, virtual material assignment on object, and others. It also can perform various industrial standard tests to aid the users in determine the expected result of their designed components. Such test is used to correct any error arises from the design.

In this project, SolidWorks will be used to design the gripper's mechanical part. The SolidWorks has various functions which will able to show the expected component design in virtual form. This program allows the user easily make changes on the dimension of their designed components. The figure 4.8 shows the SolidWorks CAD program used in this project.

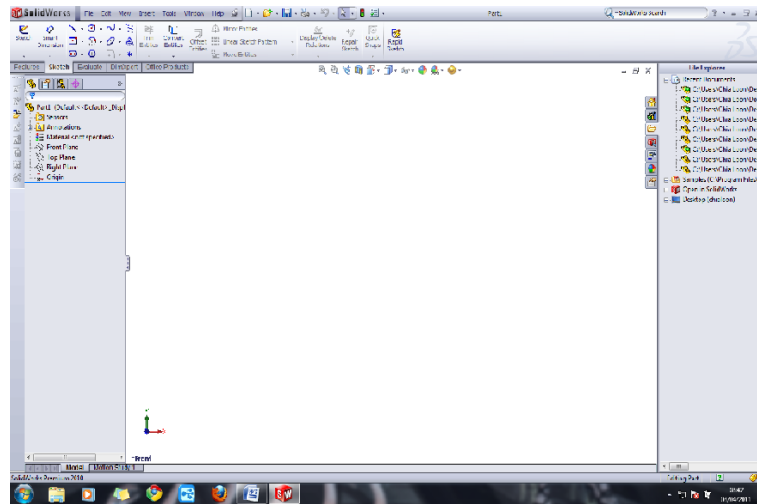


Figure 4.8: Interface of the SolidWorks program.

4.1.6 Virtual Design in SolidWorks

The mechanical structure will be designed in line with the shape of the selected conceptual design using the components selected. The mechanical structure will be drawn in the computer aided software (CAD) which is the SolidWorks.

4.1.6.1 Sensors

The position of each of the sensors will be considered thoroughly in the design of the gripper's finger. This is due to the sensors such as IRDD and IROD will be inserted into the body of the gripper's finger and such place will be drilled. Once drilled, the position cannot be undone. The IRDD will be inserted into the gripper's palm while the IROD will be installed into the pocket created at the surface of the finger's body.

4.1.6.2 General Dimension of the Finger's Body

The gripper's finger will be designed to host all the components and the sensors on it. All finger's body will have standard features such as pocket holes and wide surface to host the sensors, and open area for the movement of the joint as shown in figure 4.9.

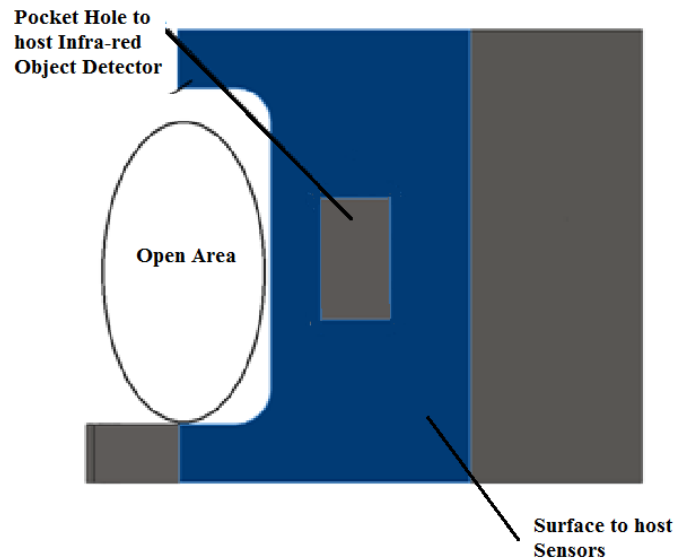


Figure 4.9: Labelling of common features of all the finger body

The height, weight and the length will be highly influenced by the dimension of the servomotor Hitec HS-56. Since the servomotor will be inserted into the body of the gripper's finger, the dimension of the body must be big enough to host the motor.

Besides that, the finger bodies' dimensions will be set to have larger dimension to accommodate the physical part of the sensors and servomotor. Figure 4.10 shows the dimension of the motor. This dimension will be used as reference to design the body dimension of gripper's finger as shown in figure 4.11 and 4.12.

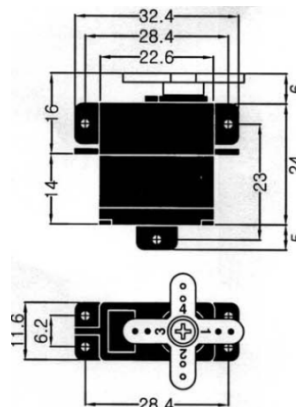


Figure 4.10: The dimension specification of the Servomotor Hitec HS-56

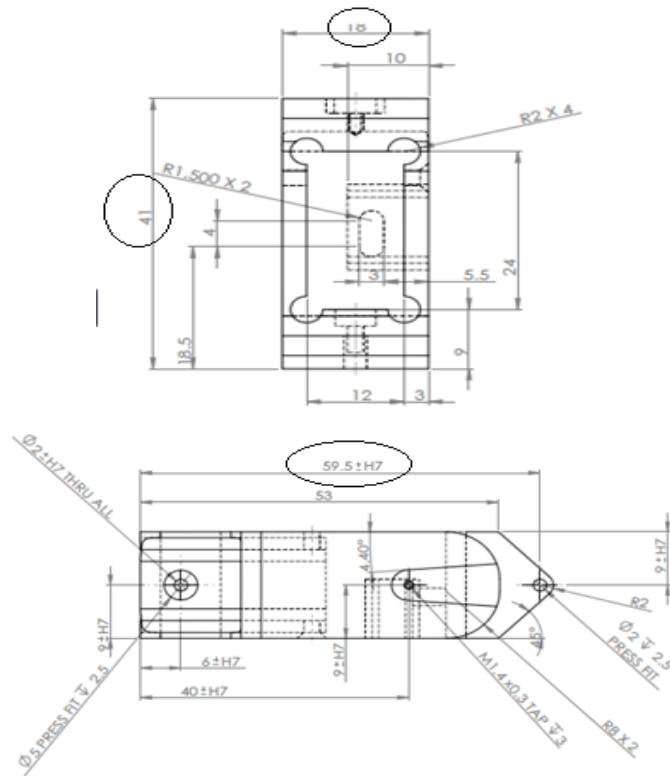


Figure 4.11: The minimum dimension of the finger body in front view and top view.

Table 8: The finger body location and length

Location	Finger Body	Length (mm)
1	Finger Tip	35
2	Thumb	47
3	Finger_Joint A	53
4	Finger_Joint B	40
5	Finger_Joint C	52.35

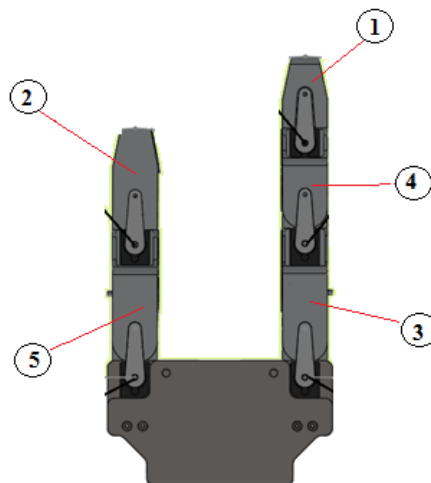


Figure 4.12: The assignment of name for each of the finger bodies.

4.1.6.3 Pocket Hole

The pocket hole drilled into the body of the fingers' body is shown in figure 4.13. The pocket hole will be used to host the servomotor in position as well as the infrared object detector. The pocket holes are drilled with references to the size of the components to be inserted. The figure 4.13 shows the pocket hole that is presented in the CAD software.

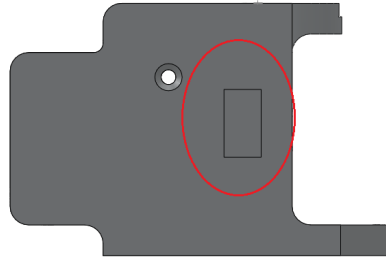


Figure 4.13: The pocket hole for the infrared object detector is circle at the thumb finger.

4.1.6.4 Bearing Housing

The bearing housing will be located at base of the finger's body. The bearing will be coupled to the dowel pin which will be press to fit which means the bearing will be tightly attached to the dowel pin. The dowel pin will be attached to the hole at the joint of the finger's base. By making the dowel pin press to fit into the bearing, the bearing will be supported by the dowel pin. The dowel pin will be supported by the body's hole as shown in figure 4.14. This will ensure the bearing will not drop during the disassembly since it is fixing to the dowel pin.

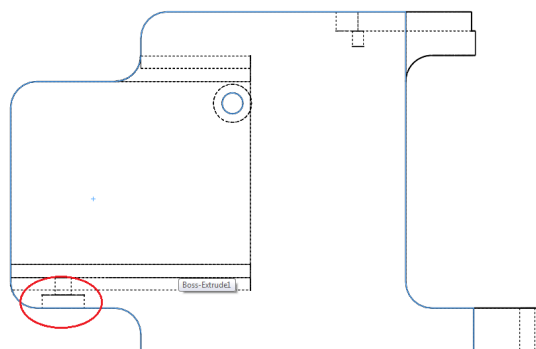


Figure 4.14: The bearing housing designed at the base of the finger body.

4.1.6.5 Coupler Housing

The coupler housing is shown in figure 4.15. The housing will be drilled to press fit which means the coupler will be fixed tight at the finger's body so it will not cause any vibration.

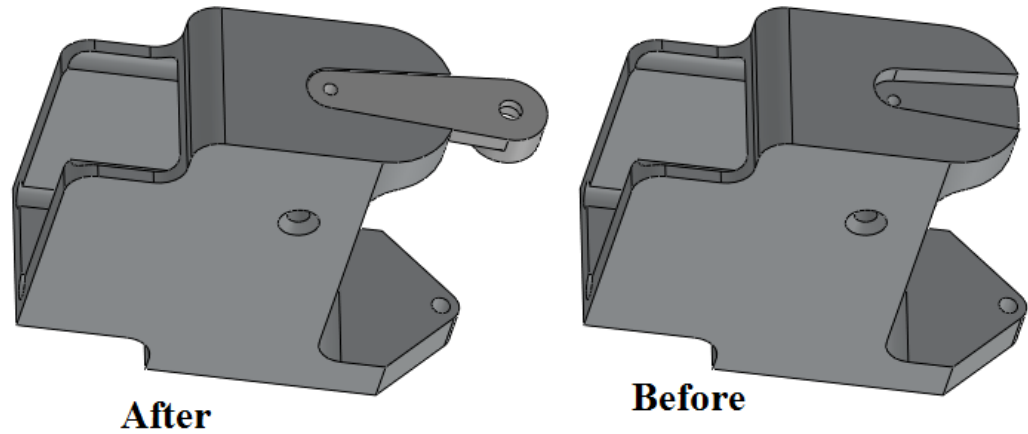


Figure 4.15: The coupler housing housed with a coupler

4.1.6.6 Radius and Fillet

Some of the important edges are made into radius shape. The radius shape located at the body joint is shown in figure 4.16.

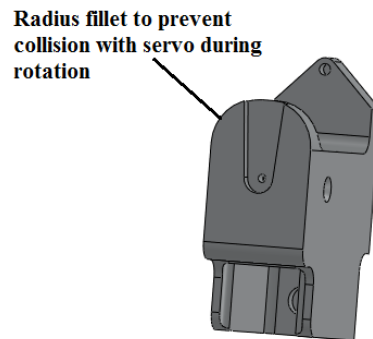


Figure 4.16: The radius fillet at the edge of finger body.

The radius of the body joint is used to maximize the turning angle of the link's joint. This can allow the finger linkage to turn in with wide degree so it can perform gripping task easily.

4.1.6.7 Palm Design

The figure 4.17 shows the virtual design of the palm. The palm design will be designed in ‘U’ shape. The ‘U’ shape palm can be used to house the IRDD and the servomotor. The ‘U’ shape palm can be fabricated out easily by bending a solid cast iron plate. This screw hole of the palm will then be machined out using the Computer Numerical Control (CNC) machine. The square area near the joint is removed to allow the turning of the servomotor’s coupler.

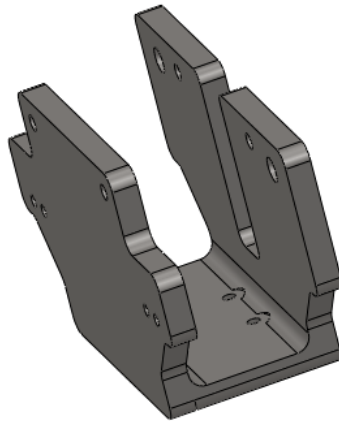


Figure 4.17: The view of palm design

4.1.6.8 Offset the Sensors in IVOARM Palm

The linear line at the middle of the base of the IVOARM palm is removed to host the IRDD as shown in figure 4.18. The IRDD contains an extruded PCB board which is needed to be addressed when placing it into the palm. The removal of the offset length is determined to be 3.5cm from the base of the gripper. This will allow the IRDD’s location to be adjusted in gripper palm.

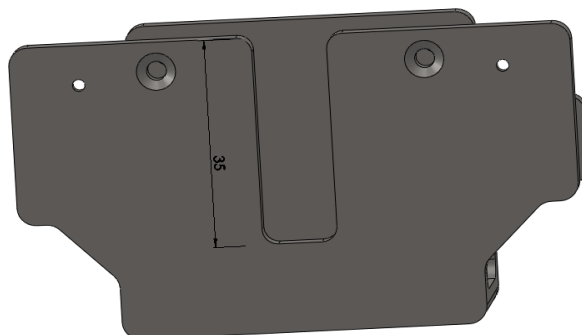


Figure 4.18: The extruded linear line at base at 35m

4.1.6.9 Foundation Settlement

The Foundation Settlement is built as shown in figure 4.19. It is used as a temporary support to hold the IVOARM gripper while performing testing. Its stand is built from existing aluminium profile which allows the cast iron plate to move up and down. The Helen screws are attached to the plate and the aluminium profile in such a way that the cast iron plate's height can be adjusted.

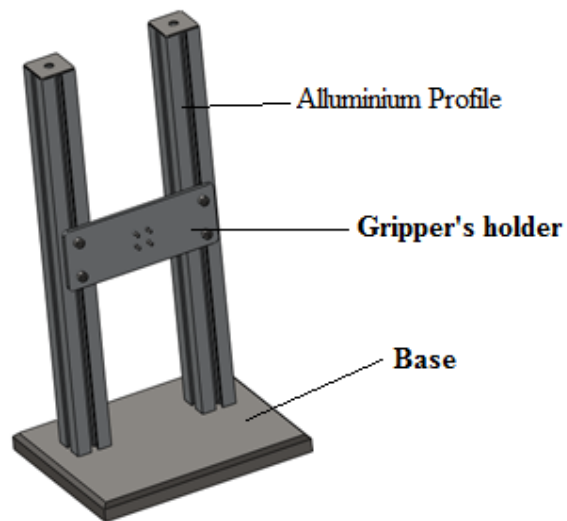


Figure 4.19: The foundation settlement in virtual display

4.1.6.10 Gripper's Virtual Assembly

4.1.6.10.1 Virtual Assembly of the Gripper's Finger

The assembly of the right gripper's finger is shown in figure 4.20 and 4.21.

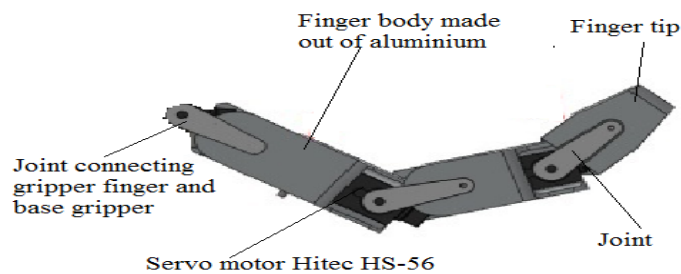


Figure 4.20: Top view of the three joint finger parts.

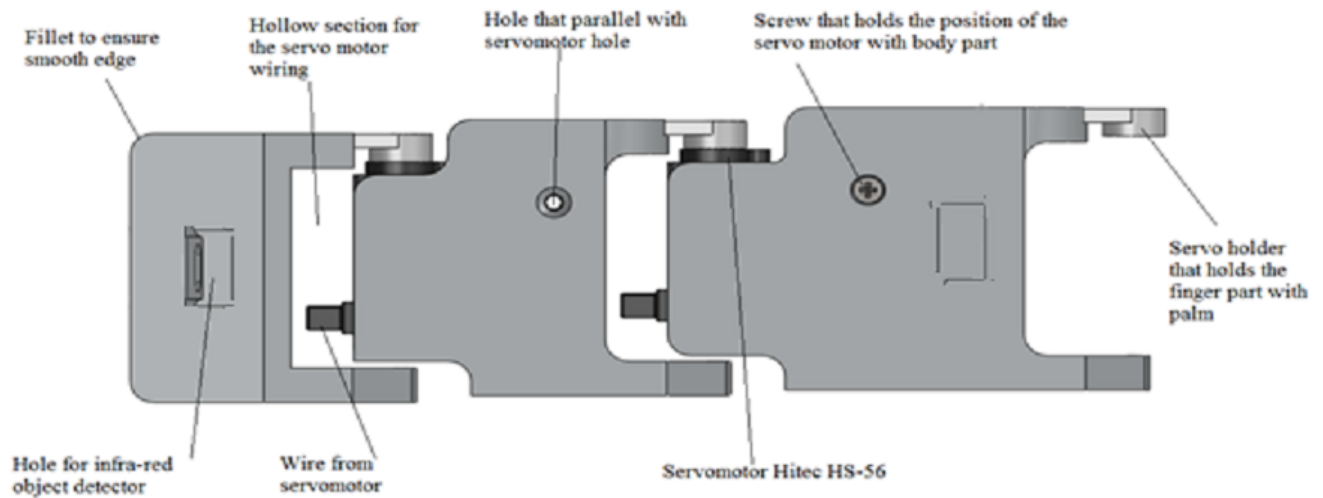


Figure 4.21: Side view of the three joint finger gripper parts

The assembly of the right gripper's finger is shown in figure 4.22 and 4.23.

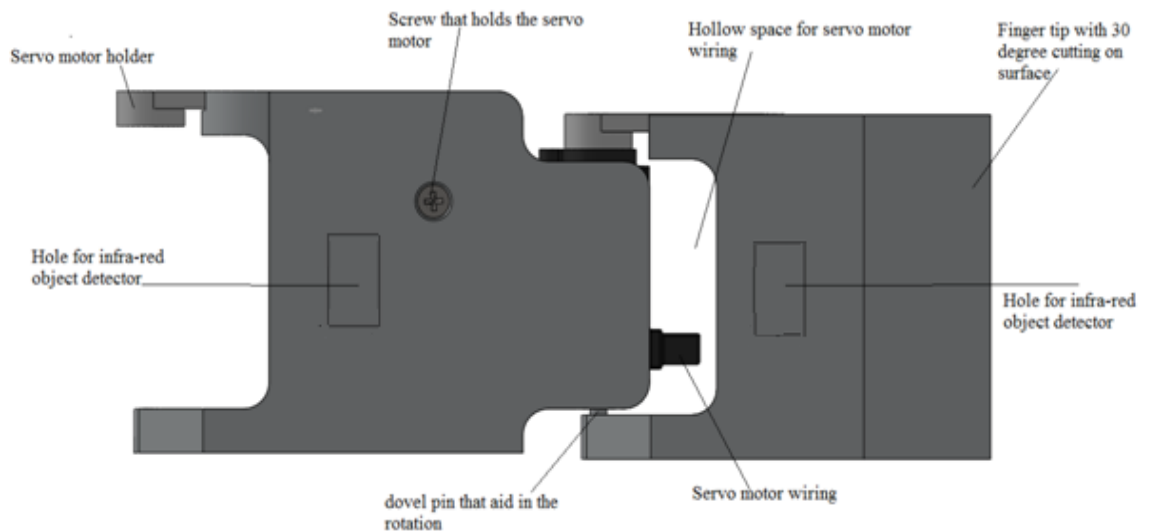


Figure 4.22: Side view of the two joint finger gripper parts.

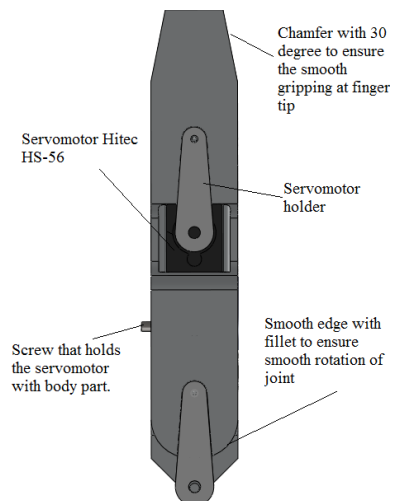


Figure 4.23: Top view of two joints finger

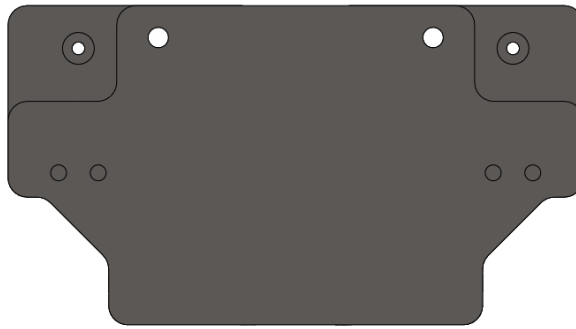


Figure 4.24: Top view of the palm of the IVOARM gripper



Figure 4.25: Side view of the palm of the IVOARM gripper.

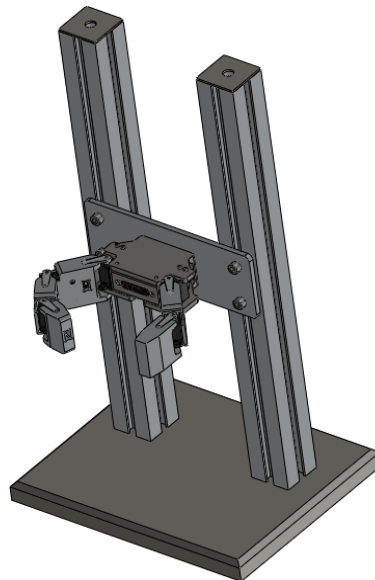


Figure 4.26: Full assembly of IVOARM gripper with foundation settlement in virtual form

The full assembly of IVOARM gripper with supporting stands as shown in figure 4.26. The foundation settlement will allow the gripper to move in horizontal motion to adjust the height.

4.1.7 Detailed Modelling

When the virtual assembly process is done, the details of the components such as movement, forces it can sustain, stress concentration, weights and others should be model out in the software as prevention against failure. It is also used to ensure all the dimension and error are within tolerated range before fabricating out the parts.

4.1.7.1 Movement of the gripper

After the assembly in virtual form, the rotational joint of gripper's fingers is tested in the Solidworks assembly window. The maximum degree of rotation of each finger joint is measured using the 'dimension tools' function. This can be used to determine the workspace of the gripper's finger and its virtual movement. Figure 4.27 shows the measurement of the gripper's maximum rotation of each finger's joint and the length measurement. The length on right finger can move 128mm radius while the length on left finger can move in 99.35mm radius. Figure 4.27 shows the illustration of IVOARM workspace using the SolidWorks Assembly function.

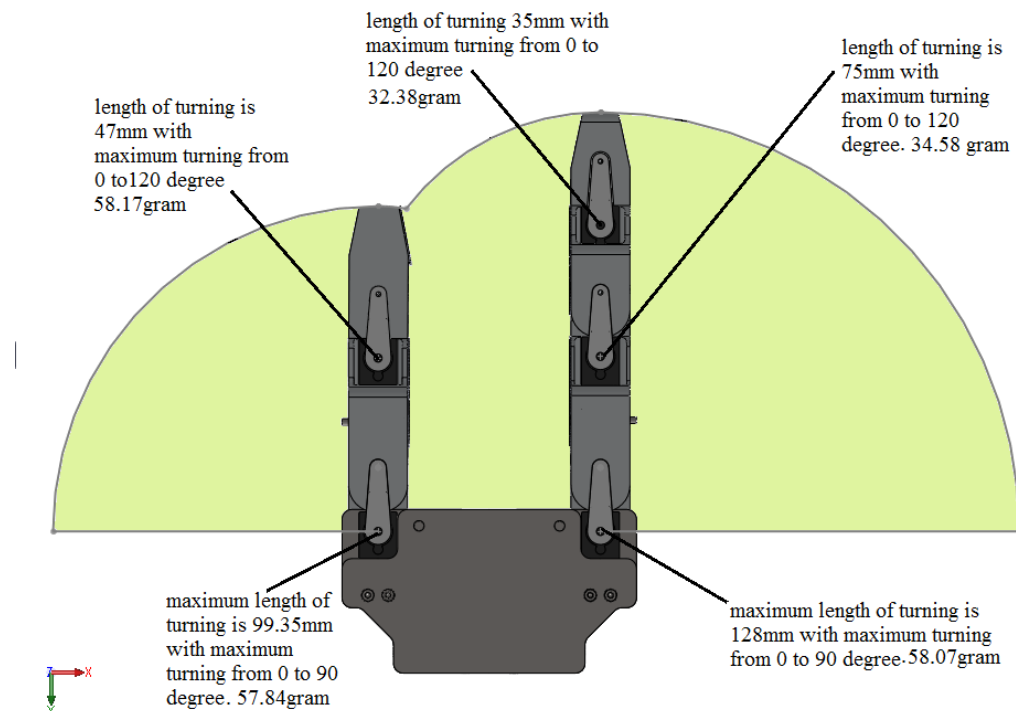


Figure 4.27: The workspace of the Gripper finger IVOARM in SolidWorks software.

4.1.7.2 Simulation of Stress Concentration Using SolidWorks

The stress simulation results in figure 4.28 to figure 4.32 are obtained during the modeling sections

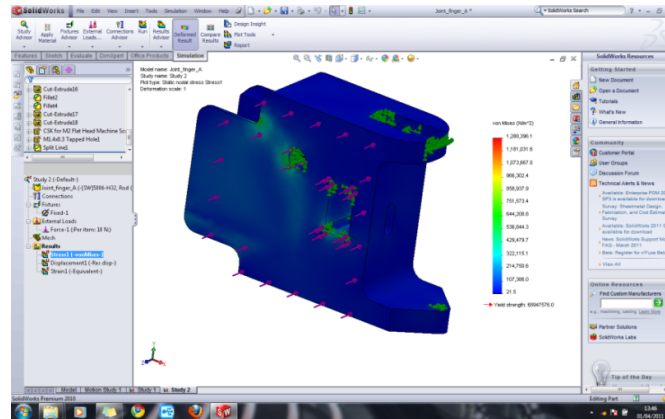


Figure 4.28: The stress concentration on the surface of the finger gripper A

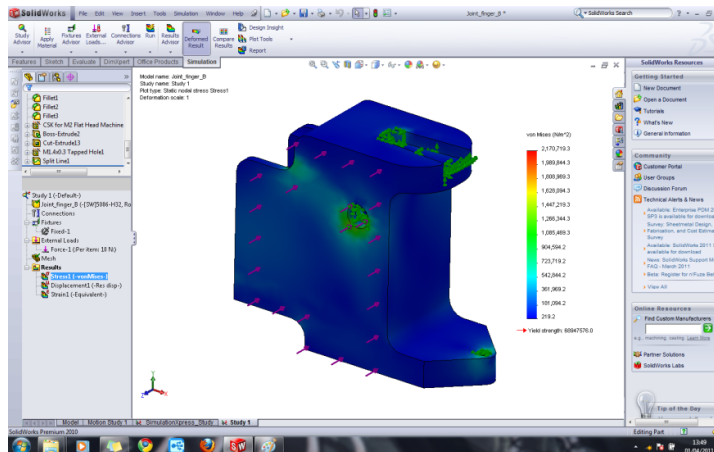


Figure 4.29: The stress concentration on the surface of the finger gripper B

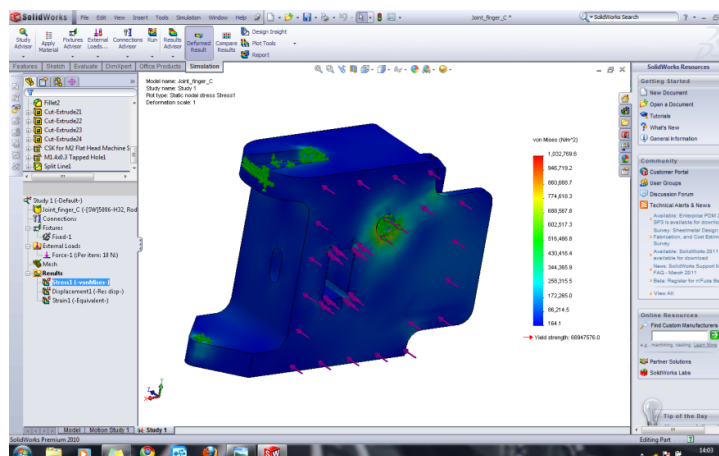


Figure 4.30: The stress concentration on the surface of the finger gripper C

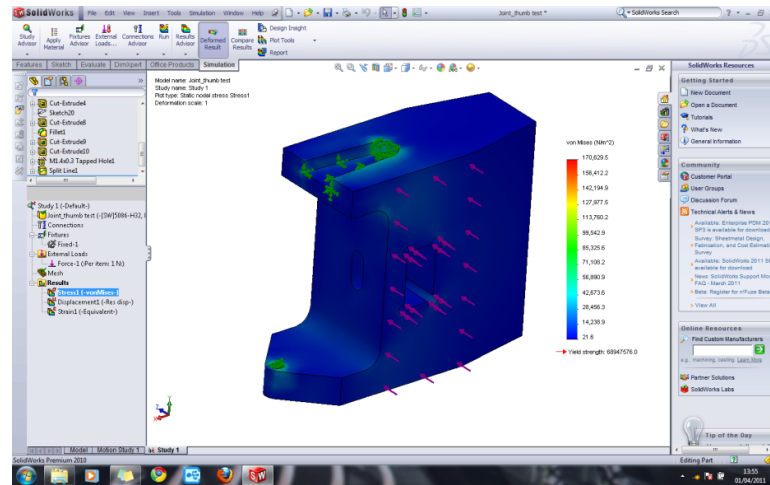


Figure 4.31: The stress concentration on the surface of the thumb

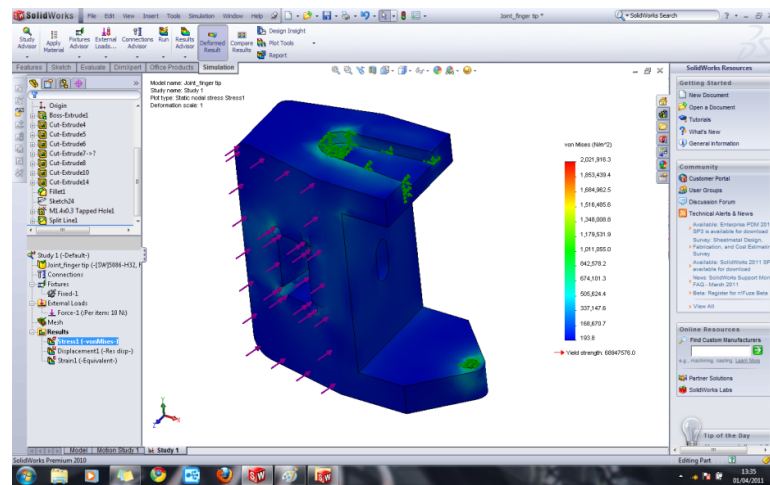


Figure 4.32: The stress concentration on the surface of the finger tip

Table 9: The stress concentration location with force applied.

Component	Force applied	Locations
Finger joint A	10Nm on the entire surface	The edge of the finger surface and the pocket hole
Finger joint B	10Nm on the entire surface	The edge of the finger surface
Finger joint C	10Nm on the entire surface	The edge of the finger surface and the pocket hole
Thumb	10Nm on the entire surface	The edge of the finger surface and the pocket hole
Finger Tip	10Nm on the entire surface	The edge of the finger surface and the pocket hole

The colours distribution in figure 4.28 to figure 4.32 has indicated the stress that the components can sustain. All the parts are subjected to maximum stress of 10Nm to have a better view of the colours distribution. All the components' surface have the blue colour distribution which indicates the surface can resist the deformation. However, most of the stresses are located at the edge of the components as shown in Table 9. This is due to its location which is situated near the empty space. The empty space allows the edge to deform towards it.

4.1.8 CAD Drawing Sent to Manufacturer.

Once the mechanical designed parts are confirmed, the CAD drawing and Build of Material (BOM) as shown in figure 4.33 and figure 4.34 will be sent to the manufacture. The manufacturer engineers will check and inform any errors on the component parts or drawing to ensure that each designed part can be fabricated out using industrial standard tools. The exploded view is shown in figure 4.35.

Bill of Material List (BOM List)

ITEM NO.	PART NUMBER	DESCRIPTION	QTY.
1	Joint_finger_A	Fabricate	1
2	servo motor	Purchase	5
3	servo holder	Purchase	5
4	palm	Fabricate	1
5	Force Sensor	Purchase	3
6	Joint_finger tip	Fabricate	1
7	Joint_thumb test	Fabricate	1
8	Joint_finger_C	Fabricate	1
9	Joint_finger_B	Fabricate	1
10	Sharp IR GP2D120	Purchase	1
11	palm 2	Fabricate	1
12	B18.6.7M - M3 x 0.5 x 30 Type I Cross Recessed	Purchase	1
13	B18.6.7M - M3 x 0.5 x 16 Type I Cross Recessed	Purchase	2
14	B18.3.1M - 10 x 1.5 x 30 Hex SHCS -- 30NHX	Purchase	1
15	ISO 4762 M6 x 10 --- 10N	Purchase	1
16	ISO 4762 M2 x 16 --- 16N	Purchase	2
17	B18.6.7M - M2 x 0.4 x 20 Type I Cross Recessed	Purchase	4
18	Infra-red Object Detector	Purchase	6

Figure 4.33: Bill of material of the IVOARM gripper

4.1.9 Feedback from the Manufacturer

Once the detailed modelling and modification has been done, the drawing files will be sent to the manufacturer which is IPE Automation Sdn. Bhd for feedback. The engineers from the IPE Company will return feedback and some recommendation to ensure the gripper design can be fabricated using industrial standard. The following is the recommendation from the IPE engineers.

4.1.10 Pocket Hole

The edges of the pocket holes are recommended to be in radius shape as shown in figure 4.36.

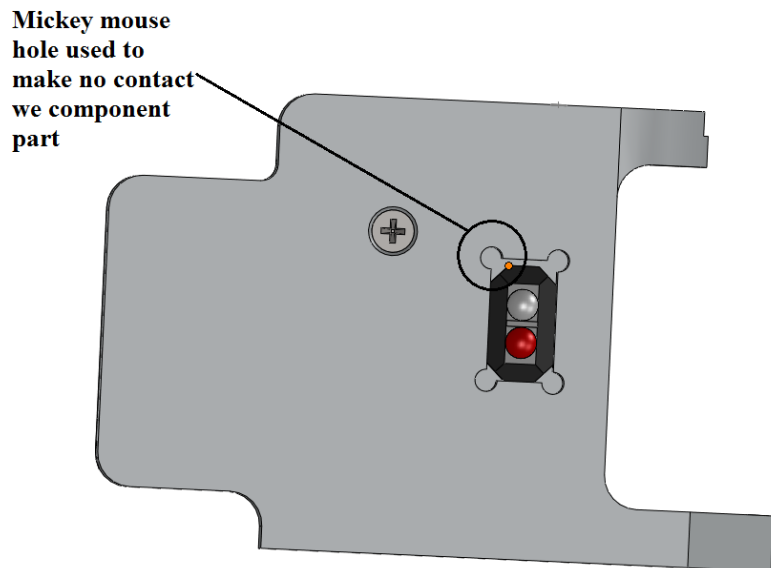


Figure 4.36: The Mickey Mouse hole drilled at the pocket holes

4.1.11 Bearing Housing

The bearing housing will be located on the top of the surface of the finger body joint as shown in the figure 4.37 and figure 4.38 shows the bearing house in 3 dimension view. The initial design of the housing is located base of the finger's body. The housing is relocated to the internal top surface of the finger body with the recommendation from the IPE.

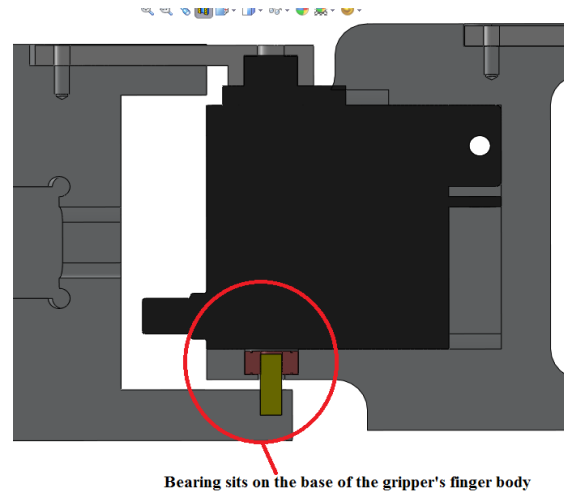


Figure 4.37: The new location of the bearing

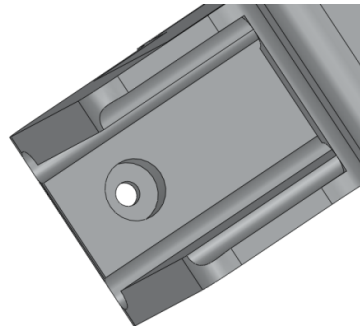


Figure 4.38: The new bearing housing location view in 3 Dimension.

4.1.12 **Palm**

The usage of block material as raw material for the palm is recommended by IPE.

4.1.13 **Screw hole**

The screw holes need to be reassigned with specific holes such as M3 flat head, M2 oval head and M3 Tap Drill. This is to standardizing the hole's dimension with the industrial level.

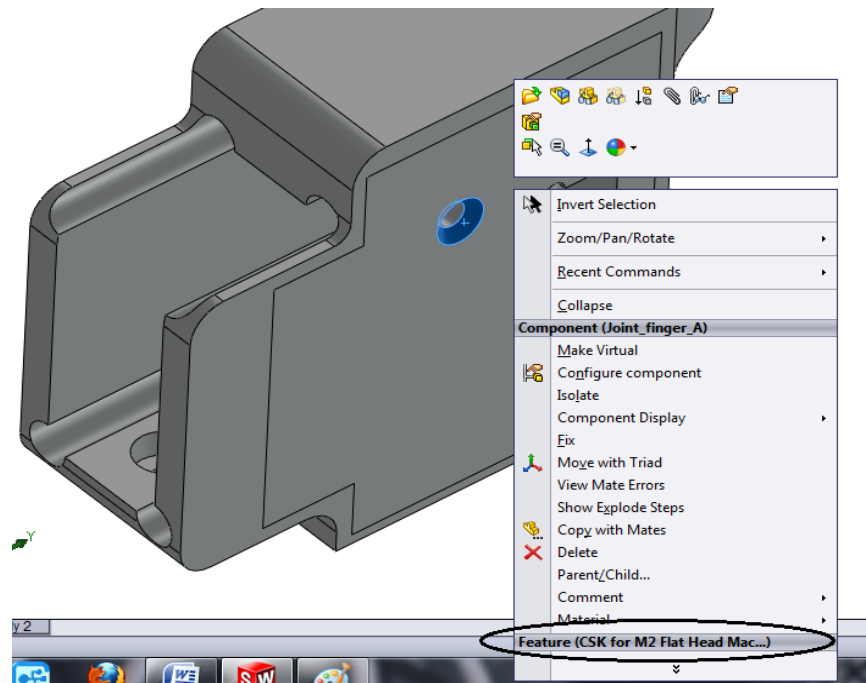


Figure 4.39: The CSK screw hole that support the servomotor with finger body

4.1.14 CAD Drawing

The readjustment of the CAD drawing dimensions have been urged by IPE engineers. The important dimension such as 24 mm is more important than 5mm plate shown on the right in figure 4.40.

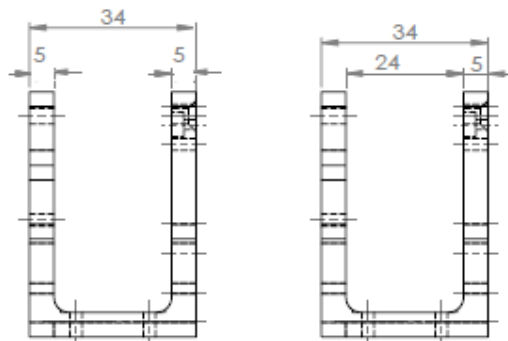


Figure 4.40: Two 'U' shape palm with different labelling

4.1.15 Dowel pin.

The IPE recommend the dowel pin used in design should be custom made with slight angle at the tip rather than purchasing the dowel pin in the market.

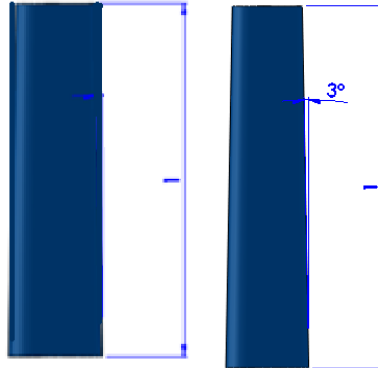



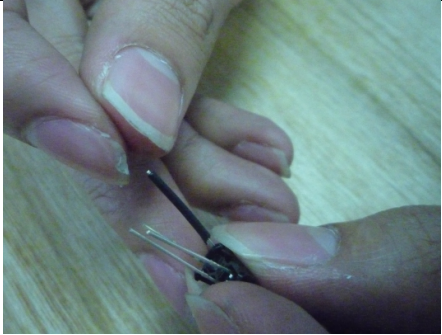
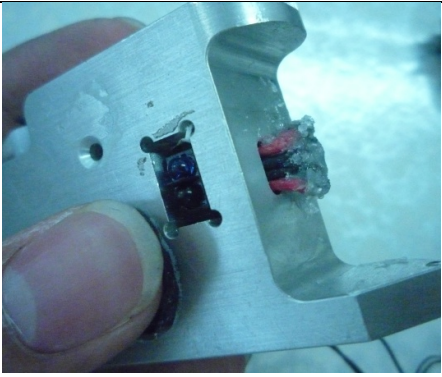

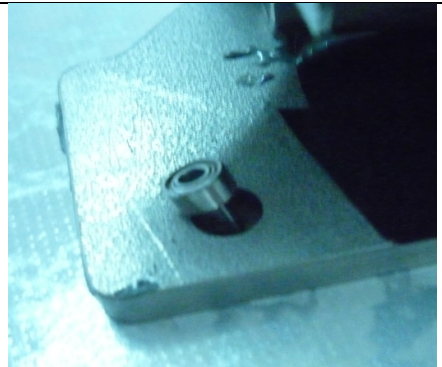

Figure 4.41: The thin rod dowel pin on the left side and the dowel pin with angle on right side

The recommendation is heeded and new CAD drawing will be sent to IPE Automation Sdn. Bhd for final checking and fabrication.

4.2 Assembly of Component Parts

The parts are collected from manufacturer and assembled as shown in figure 4.42. The parts are examined to ensure the dimension and shapes are following the dimensions as stated in the CAD drawing. Once the dimension is confirmed, the parts are assembled to test its mechanical movement of the gripper's finger, and the installation of the sensors. Once the mechanical movement and the installation of the sensors are validated, the designing process is now end.

Assembly Figure	Description
	<p>Mechanical parts of the gripper received from the IPE manufacturer.</p>

	<p>The infrared object detector is inserted with rubber cover as protection</p>
	<p>The infrared object detector is inserted into the pocket hole and the wire is seal with silicon glue.</p>
	<p>The dowel pin is inserted into the bearing</p>
	<p>The bearing with dowel pin is inserted into the bearing housing</p>
	<p>The servomotor is inserted into the finger body</p>

	<p>The servo holder is fixed at both finger body and the holder itself.</p>
	<p>The gripper fingers are fit with servomotor all the servomotors</p>
	<p>The L-shape plate is attached at the side of servomotor at palm to prevent it from vibrating while rotates.</p>
	<p>The final attachment at the foundation settlement with force sensors and IROD</p>

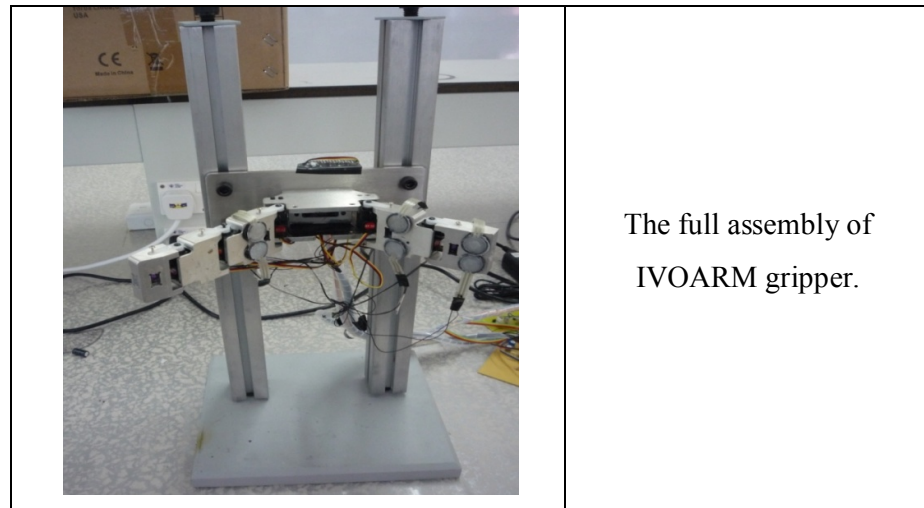
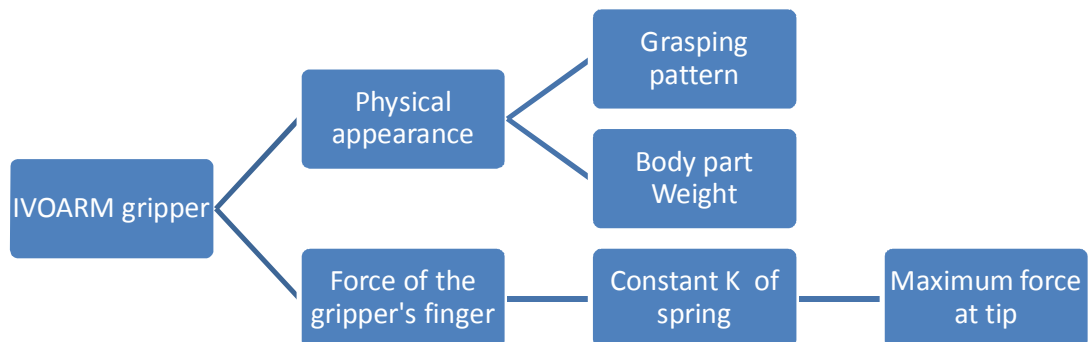


Figure 4.42: The assembly step by step of IVOARM

4.3 Test and Validate Through Experiment

4.3.1 Overview of the Mechanical Design Experiment



The fabricated IVOARM will undergo small experiment to verify its characteristic. The IVOARM will undergo the verification of grasping pattern and weight of the body part with simulation.

Besides that, the maximum force at tip will be indentified. It will be verified with calculation. The experiment on constant K is to aid the experiment of maximum force at tip in which the spring will be used to obtain the force.

4.3.2 Experiment Method

An experiment using elongation of spring method is used to test the maximum force that can be sustained at the finger tip. The spring is tested with various loads to obtain the spring constant. Once the spring constant is determined, the spring will now be attached to the finger tip or thumb. The whole finger tip will be rotate to the direction against the spring. The elongation of the spring will be recorded to calculate the maximum force of the gripper's finger can sustain in real IVOARAM gripper. These results will be verified with the calculated value.



Figure 4.43: Experiment on spring to obtain the constant, k .



Figure 4.44: Spring is subject to elongation from the rotation of the gripper's finger which pulls the spring.

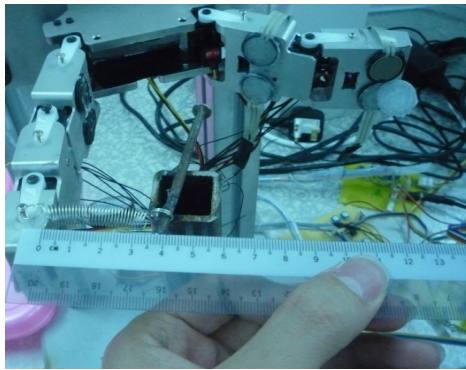


Figure 4.45: The spring is measured to determine the force at tip.

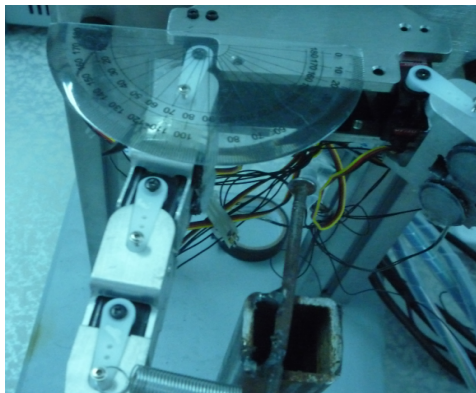


Figure 4.46: Angle is taken as the same time with measurement of spring at tip

4.3.3 Maximum Force at Tips

The formulation force and torque propagation needed to be done before the experiment takes place. This equation will be used to calculate the theoretical force and verify the experimented force.

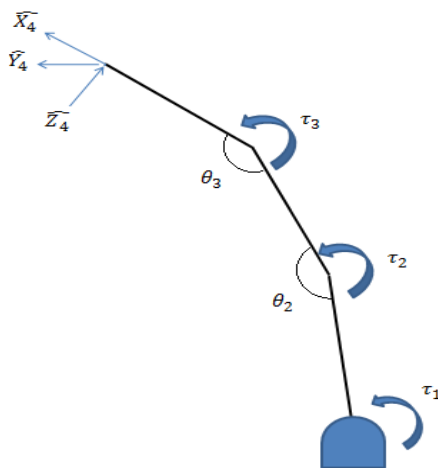


Figure 4.47: The kinematic of three joint to formulate static force and torque propagation

Table 10: David-Hartenberg Table

i	α_{i-1}	a_{i-1}	d_i	θ_i
1	0	0	0	θ_1
2	l_3	0	0	θ_2
3	l_2	0	0	θ_3
4	l_1	0	0	0

$${}^0T_1 = \begin{bmatrix} C_1 & -S_1 & 0 & 0 \\ S_1 & C_1 & 0 & 0 \\ 0 & 0 & 1 & 0 \\ 0 & 0 & 0 & 1 \end{bmatrix} \quad (12)$$

$${}^1T_2 = \begin{bmatrix} C_1 & -S_1 & 0 & 0 \\ S_1 & C_1 & 0 & 0 \\ 0 & 0 & 1 & 0 \\ 0 & 0 & 0 & 1 \end{bmatrix} \quad (13)$$

$${}^2T_3 = \begin{bmatrix} C_1 & -S_1 & 0 & 0 \\ S_1 & C_1 & 0 & 0 \\ 0 & 0 & 1 & 0 \\ 0 & 0 & 0 & 1 \end{bmatrix} \quad (14)$$

$${}^3T_4 = \begin{bmatrix} 1 & 0 & 0 & 0 \\ 0 & 1 & 0 & 0 \\ 0 & 0 & 1 & 0 \\ 0 & 0 & 0 & 1 \end{bmatrix} \quad (15)$$

Force and torque at tip

$${}^4f_4 = \begin{bmatrix} f_x \\ f_y \\ 0 \end{bmatrix} \quad (16)$$

$${}^4n_4 = 0 \quad (17)$$

Force and torque at third link

$${}^3f_3 = \begin{bmatrix} 1 & 0 & 0 \\ 0 & 1 & 0 \\ 0 & 0 & 1 \end{bmatrix} \begin{bmatrix} f_x \\ f_y \\ 0 \end{bmatrix} = \begin{bmatrix} f_x \\ f_y \\ 0 \end{bmatrix} \quad (18)$$

$${}^3n_3 = \begin{bmatrix} 1 & 0 & 0 \\ 0 & 1 & 0 \\ 0 & 0 & 1 \end{bmatrix} \begin{bmatrix} 0 \\ 0 \\ 0 \end{bmatrix} + \widehat{X}_3 l_3 \times \begin{bmatrix} f_x \\ f_y \\ 0 \end{bmatrix} = \begin{bmatrix} 0 \\ 0 \\ l_3 f_y \end{bmatrix} \quad (19)$$

Force and torque at second link

$${}^2f_2 = \begin{bmatrix} C_3 & -S_3 & 0 \\ S_3 & C_3 & 0 \\ 0 & 0 & 1 \end{bmatrix} \begin{bmatrix} f_x \\ f_y \\ 0 \end{bmatrix} = \begin{bmatrix} f_x C_3 - f_y S_3 \\ f_x S_3 + f_y C_3 \\ 0 \end{bmatrix} \quad (20)$$

$${}^2n_2 = \begin{bmatrix} C_3 & -S_3 & 0 \\ S_3 & C_3 & 0 \\ 0 & 0 & 1 \end{bmatrix} \begin{bmatrix} 0 \\ 0 \\ l_3 f_y \end{bmatrix} + \begin{bmatrix} l_2 \\ 0 \\ 0 \end{bmatrix} X \begin{bmatrix} f_x C_3 - f_y S_3 \\ f_x S_3 + f_y C_3 \\ 0 \end{bmatrix} \quad (21)$$

$$= \begin{bmatrix} 0 \\ 0 \\ l_3 f_y \end{bmatrix} + \begin{bmatrix} 0 \\ 0 \\ l_2 (f_x S_3 + f_y C_3) \end{bmatrix} \quad (22)$$

$$= \begin{bmatrix} 0 \\ 0 \\ l_3 f_y + l_2 (f_x S_3 + f_y C_3) \end{bmatrix} \quad (23)$$

Force and torque at first link

$${}^1f_1 = \begin{bmatrix} C_2 & -S_2 & 0 \\ S_2 & C_2 & 0 \\ 0 & 0 & 1 \end{bmatrix} \begin{bmatrix} f_x C_3 - f_y S_3 \\ f_x S_3 + f_y C_3 \\ 0 \end{bmatrix} \quad (24)$$

$$= \begin{bmatrix} f_x C_3 C_2 - f_y S_3 C_2 - f_x S_3 S_2 - f_y S_2 C_3 \\ f_x C_3 S_2 - f_y S_3 S_2 + f_x S_3 C_2 + f_y C_2 C_3 \\ 0 \end{bmatrix} \quad (25)$$

$${}^1n_1 = \begin{bmatrix} C_2 & -S_2 & 0 \\ S_2 & C_2 & 0 \\ 0 & 0 & 1 \end{bmatrix} \begin{bmatrix} 0 \\ 0 \\ l_3 f_y + l_2 (f_x S_3 + f_y C_3) \end{bmatrix} +$$

$$\begin{bmatrix} l_1 \\ 0 \\ 0 \end{bmatrix} X \begin{bmatrix} f_x C_3 C_2 - f_y S_3 C_2 - f_x S_3 S_2 - f_y S_2 C_3 \\ f_x C_3 S_2 - f_y S_3 S_2 + f_x S_3 C_2 + f_y C_2 C_3 \\ 0 \end{bmatrix} \quad (26)$$

$$= \begin{bmatrix} 0 \\ 0 \\ l_3 f_y + l_2 (f_x S_3 + f_y C_3) \end{bmatrix} + \begin{bmatrix} 0 \\ 0 \\ l_1 (f_x C_3 S_2 - f_y S_3 S_2 + f_x S_3 C_2 + f_y C_2 C_3) \end{bmatrix} \quad (27)$$

$$= l_3 f_y + l_2 (f_x S_3 + f_y C_3) + l_1 (f_x C_3 S_2 - f_y S_3 S_2 + f_x S_3 C_2 + f_y C_2 C_3) \quad (28)$$

The torque, τ of Joint 3 will be 1n_1 .

CHAPTER 5

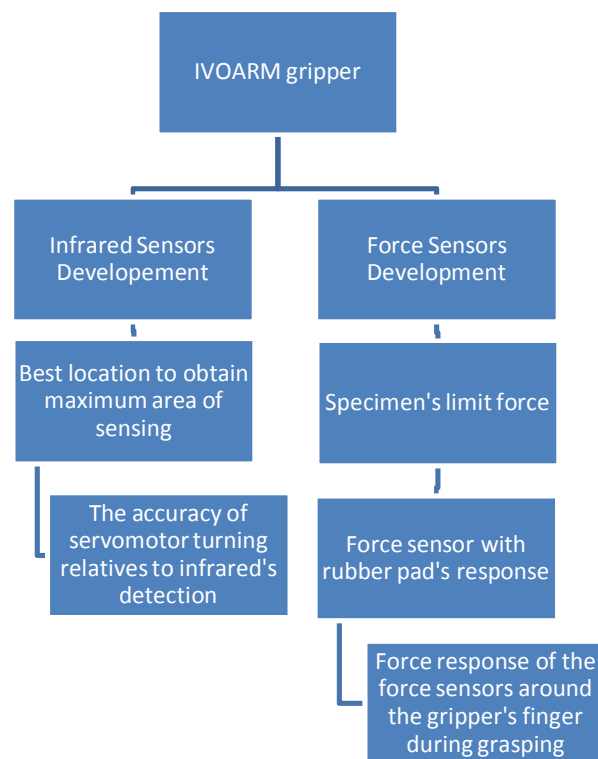
SENSOR DEVELOPEMENT5.1 **Overview of the Sensor Development Experiment**

Figure 5.1: The experiment flow chart for the Sensor Development

The sensors attached at gripper's finger will undergo some experiment related to their efficiency during the operation as shown in figure 5.1.

Infrared sensors will be tested with servomotor. During searching the object, the infrared sensors will stop the servomotor from turning if it has detected the object. The angle of turning of the servomotor will be compared with the simulated result from CAD software.

The force sensors will undergo small experiment where the specimen will first be determined. Then, the force sensor's sensitivity will be adjusted by adding rubber pad to accommodate the force limit that the specimen can sustain. An experiment on force response of the force sensors around the gripper will be determined during the grasping.

5.2 Infrared Sensors Development

5.2.1 Location of Infrared sensors

The locations of the infrared sensors are determined to gain the maximum sensing area. The sensing area of the sensor will be formed based on the polygon area. The position of each sensor will be recorded. Since the gripper finger is moving, the position and the coordination of the sensor will move as well. Therefore, a polygon area using the coordinate system which is the Beyer polygon theory is used.

5.2.2 Beyer's Polygon Area

The equation shown here is the derivation using the Beyer polygon theory as shown in (11). Since there are 5 infrared sensors, the equation will be:

$$A = \frac{1}{2} \left(\left| \begin{matrix} X_1 & X_2 \\ Y_1 & Y_2 \end{matrix} \right| + \left| \begin{matrix} X_2 & X_3 \\ Y_2 & Y_3 \end{matrix} \right| + \left| \begin{matrix} X_3 & X_4 \\ Y_3 & Y_4 \end{matrix} \right| + \left| \begin{matrix} X_4 & X_5 \\ Y_4 & Y_5 \end{matrix} \right| + \left| \begin{matrix} X_5 & X_1 \\ Y_5 & Y_1 \end{matrix} \right| \right) \quad (29)$$

$$A = \frac{1}{2} (X_1Y_2 - X_2Y_1 + X_2Y_3 - X_3Y_2 + X_3Y_4 - X_4Y_3 + X_4Y_5 - X_5Y_4 + X_5Y_1 - X_1Y_5) \quad (30)$$

Where the X_i = X coordinate system of the sensor's position

Y_i = Y coordinate system of the sensor's position

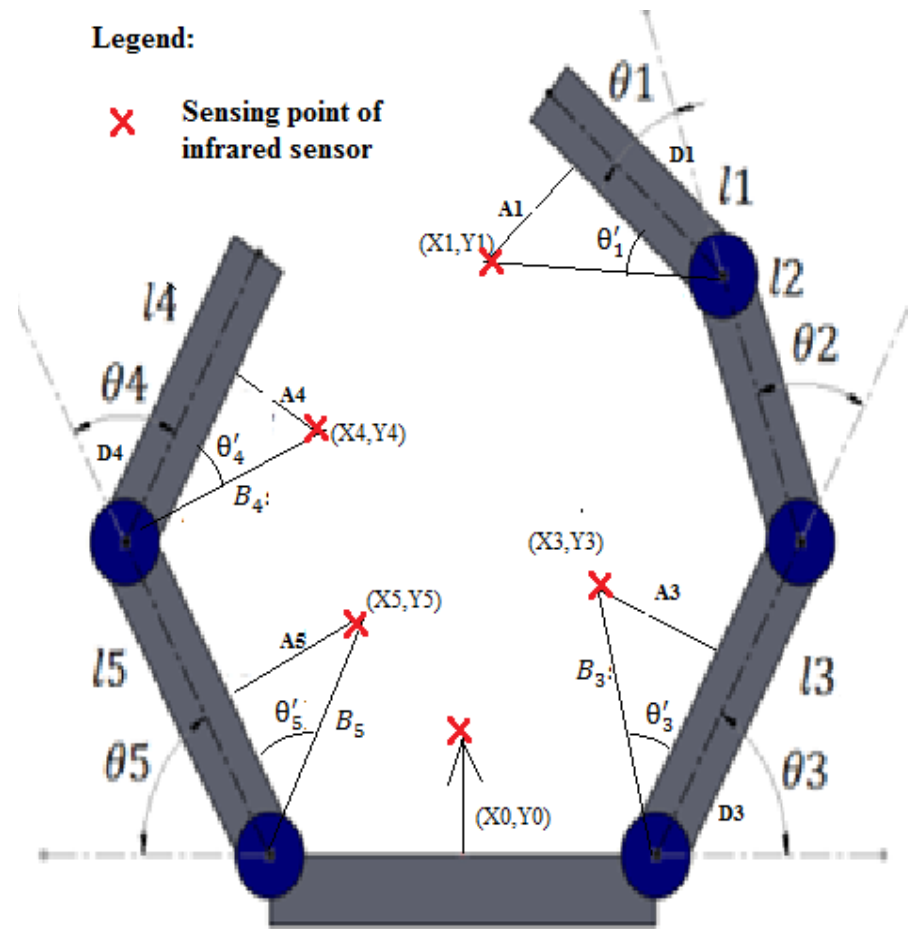


Figure 5.2: The actual sensing points of the IROD and the IRDD in IVOARM

However, in order to find the sensing position of each IROD and the IRDD, the sensing range is needed to be known. Figure 5.2 shows the A_i which is the sensing range for the IROD. By using this A_i , each of offset of the ‘virtual link’ is now computed. This ‘virtual link’ is the length of the sensing point relatives to its joint. For example, the link 5 is offset θ'_5 degree which makes the ‘virtual link’ to be B_5 . This ‘virtual link’ is important as it is representing the kinematic link of the actual sensing point.

Using the forward kinematic in (7), (8), (9) and (10), the position of each sensing point can be calculated. Let’s take A as the variable input sensing range by the user to. Now, each of the IROD sensors has its own length position relative to the joints.

Sensor position at the link 3 relative to the joint 3 is D_3 .

Sensor position at the link 5 relative to the joint 5 is D_5 .

Sensor position at the link 4 relative to the joint 4 is D_4 .

Sensor position at the link 1 relative to the joint 1 is D_1 .

Now, using this data, formula in (14) and (15) will be form for the B and θ' using trigonometry.

$$\tan\theta'_i = \frac{A}{D_i} \quad (31)$$

$$B_i = \cos^{-1} \frac{S_i}{\theta'_i} \quad (32)$$

Where

B_i = 'virtual link',

θ'_i = offset degree from the respective joint

Using the value of B_i and θ'_i , it will be substituted into the forward kinematic in (7), (8), (9), and (10).

For 'virtual sensing' point for sensor at link 1

$$l_1 = B_1 \quad (33)$$

The length for the rest is same.

$$x1 = l_3 \cos(\theta_3 + \theta'_1) + l_2 \cos(\theta_2 + \theta_3 + \theta'_1) + B_1 \cos(\theta_1 + \theta_2 + \theta_3 + \theta'_1) \quad (34)$$

$$y1 = l_3 \sin(\theta_3 + \theta'_1) + l_2 \sin(\theta_2 + \theta_3 + \theta'_1) + B_1 \sin(\theta_1 + \theta_2 + \theta_3 + \theta'_1) \quad (35)$$

Where θ'_1 is an offset angle from the sensing range.

For 'virtual sensing' point for sensor at link 3

$$l_1 = B_3 \quad (36)$$

The length for the rest is same.

$$x3 = B_3 \cos(\theta_3 + \theta'_3) \quad (37)$$

$$y3 = B_3 \sin(\theta_3 + \theta'_3) \quad (38)$$

Where θ'_3 is an offset angle from the sensing range.

For 'virtual sensing' point for sensor at link 5,

$$l_5 = B_5 \quad (39)$$

$$x5 = B_5 \cos(\theta_5 + \theta'_5) \quad (40)$$

$$y5 = B_5 \sin(\theta_5 + \theta'_5) \quad (41)$$

Where θ'_5 is an offset angle from the sensing range.

For ‘virtual sensing’ point for sensor at link 4,

$$l_4 = B_4 \quad (42)$$

$$x_4 = B_4 \cos(\theta_4 + \theta'_4) + l_5 \cos(\theta_4 + \theta'_4 + \theta_5) \quad (43)$$

$$y_4 = B_4 \sin(\theta_4 + \theta'_4) + l_5 \sin(\theta_4 + \theta'_4 + \theta_5) \quad (44)$$

Where θ'_4 is an offset angle from the sensing range.

Each of the X coordinate on the left side relatives to the home coordinates which is (X0,Y0) needs to deduct 45 millimetre and the X coordinate on the right needs to add 45millimetre respectively because the (X0,Y0) is used as the reference coordinates.

Using this coordinates form from kinematic; maximum area of infrared sensing relatives to the movement and position of the finger can be found.

5.3 The Accuracy of Servomotor’s Angle of Turning Relatives to Infrared Object Detector

Once the best position of the infrared sensors are determined, it is necessary to determine the accuracy of the angle of turning of each of the servomotors relatives to the IROD sensor on the gripper.

The servomotor’s angle of turning is important as it will determine the results of kinematic motion in real time. An experiment will be conducted to measure the turning angle of the servomotors on the gripper’s finger when the IRODs have detected the objects presence.

Simulation on the angle of the servomotor will be conducted by setting the IROD sensing range and measure the angle on each of the servomotors during the detection of object. Once the data is collected from the experiments, it will be compared with simulation result as shown in figure 5.3.

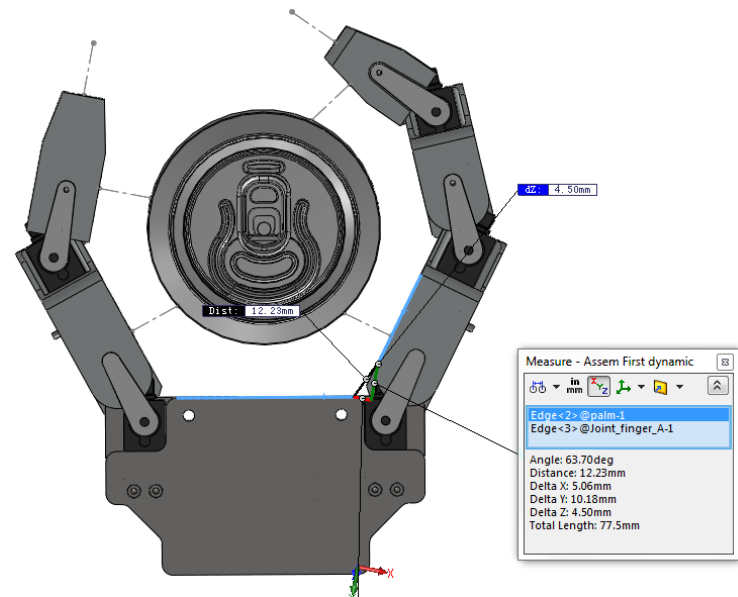


Figure 5.3: Simulation result on angle of rotation. The IROD sensing range is fixed.

5.4 Force Sensor Development

5.4.1 Force Response

The basic idea behind the stable grasping force is

Maximum force applied from gripper < Maximum force limit of the object's surface

If the maximum force applied from the gripper is higher than the maximum force limit of the object's surface, the object will break or crushed.

5.4.2 Experiment on Specimens

Three specimens will be selected which is pen, egg and can. This specimen will be put into the INSTRON 5582 machine as shown in 5.4 to obtain the force that it can sustain. The force obtained will be used as a standard reference to configure the force sensors sensing range.



Figure 5.4: The INSTRON 5582 machine used to test the maximum force onto specimens

5.4.3 Experiment on Force Sensors' Response.

Each of the force sensors will be tested to determine its sensing sensitivity. The sensing sensitivity of the FSR has been displayed in the datasheet and varies as the applied force increased.

In this project, the sensing sensitivity is important to grasp the brittle object. The FSR used in this project will be reinforced with the rubber pad to increase its sensitivity as shown in figure 5.5. It will be done by focus all the constant force applied into a small area and when the area is small, the pressure will increase as shown in formula below. Since the pressure will be relatives to the resistivity of the FSR, it will also increase the voltage output. The figure 5.5 shows the experiment of getting individual force response.

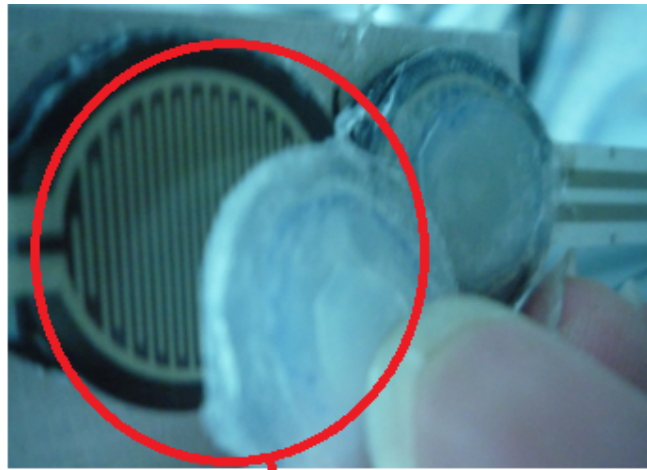
$$P = \frac{F}{A}$$

Where

P = Pressure

F=Force Applied

A= Area



Sticking rubber pad onto FSR

Figure 5.5: The surface of the FSR which is reinforced with the rubber pad.

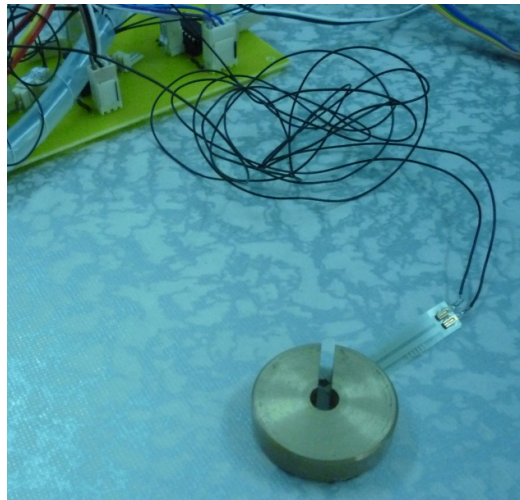


Figure 5.6: The experiment of getting FSR individual force response. FSR is applied with a load.

5.5 Experiment on the FSR's voltage output level relative to the location it locates in the gripper's finger.

The experiment of force response of the FSR on the gripper's finger while gripping will be done to determine the voltage level output of FSR. The FSR assigned to different location on the finger gripper will have different level of voltage output as the force resulted from the gripper's finger is related from its distance to the base of the joint 3 or joint 5. Figure 5.7 shows the joint assignment and the location of the FSRs. Figure 5.8 shows the object is being grasped with FSR attached.

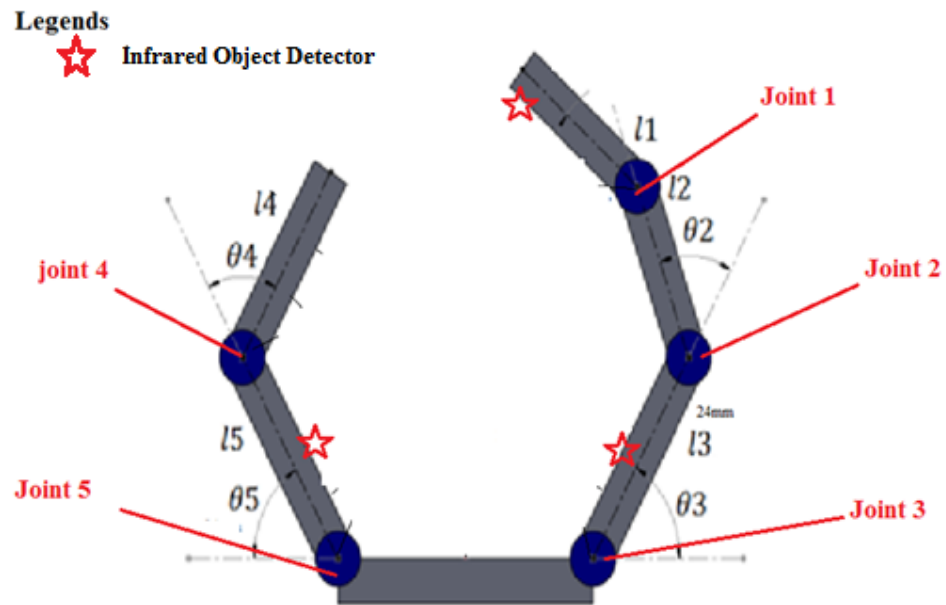


Figure 5.7: The joint's number and the sensor's location.

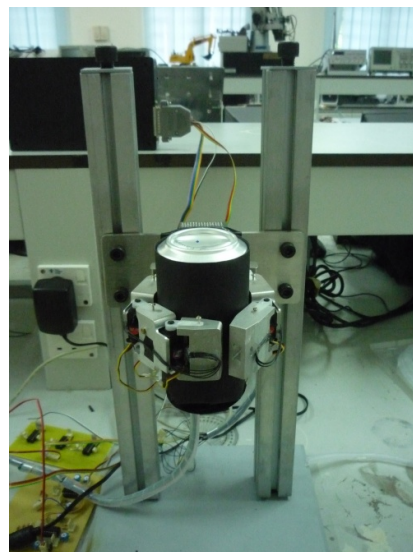


Figure 5.8: The experiment on grasping an object and measuring the FSR force response.

CHAPTER 6

RESULTS AND DISCUSSIONS**6.1 Mechanical Design****6.1.1 Body Part Weight**

The components parts received from the manufacturer's fabrication are weighted. The result is shown in Table 11.

Table 11: Comparison between actual weight and simulated weight in Solidworks

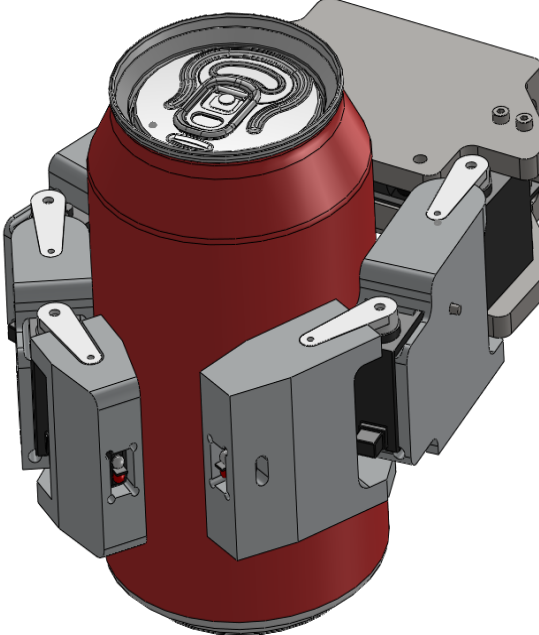
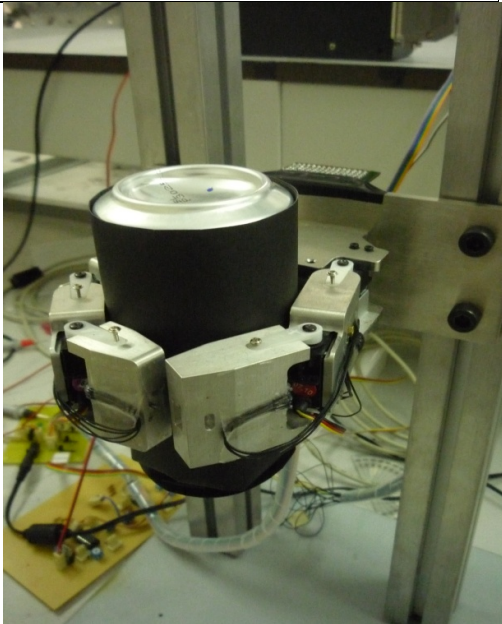
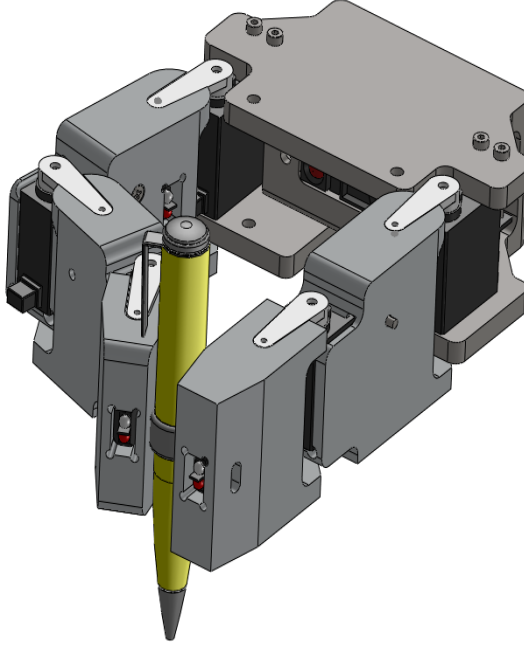
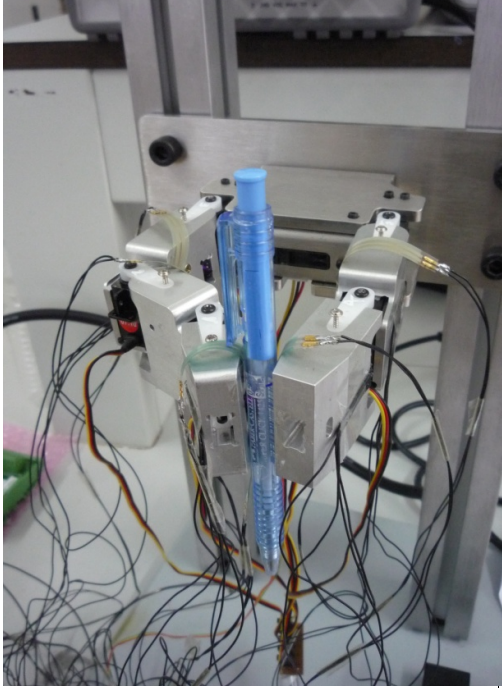
Components	Simulated Weight in CAD (gram)	Actual Weight (gram)	Error Difference (%)
Finger joint A	58.07	57.7	0.63
Finger joint B	34.58	35.1	0.15
Finger joint C	57.84	56.4	-2.49
Thumb	58.17	59.1	1.59
Finger Tip	32.38	32.1	-0.86

Discussion

The components parts' weight received from the fabrication are almost same with the simulated weight. This is due to most of the parts are fabricated using the CNC machines which has high accuracy in machining the features.

The errors arises from the fabrication is due to some features which are done by using human hand such as finishing, drilling the screw holes and others. This will not affect much since its error relatives to simulation's value is small.

6.2 Result on Pattern Grasping

Simulated Grasping Method	Actual Grasping Result
 A 3D CAD simulation showing a red cylindrical can being held by a grey robotic gripper. The gripper has four fingers, two on each side, which are positioned around the can. The can has a white logo on its top surface.	 A photograph of a physical robotic gripper holding a black cylindrical can. The gripper is mounted on a metal frame, and various wires and components are visible in the background.
Can grasping in CAD software	Can grasping in experiment
 A 3D CAD simulation showing a yellow pen being held by a grey robotic gripper. The gripper's fingers are positioned around the pen, demonstrating its ability to grasp a smaller, more delicate object.	 A photograph of a physical robotic gripper holding a blue pen. The gripper is mounted on a metal frame, and various wires and components are visible in the background.
Pen grasping in CAD software	Pen grasping in experiment

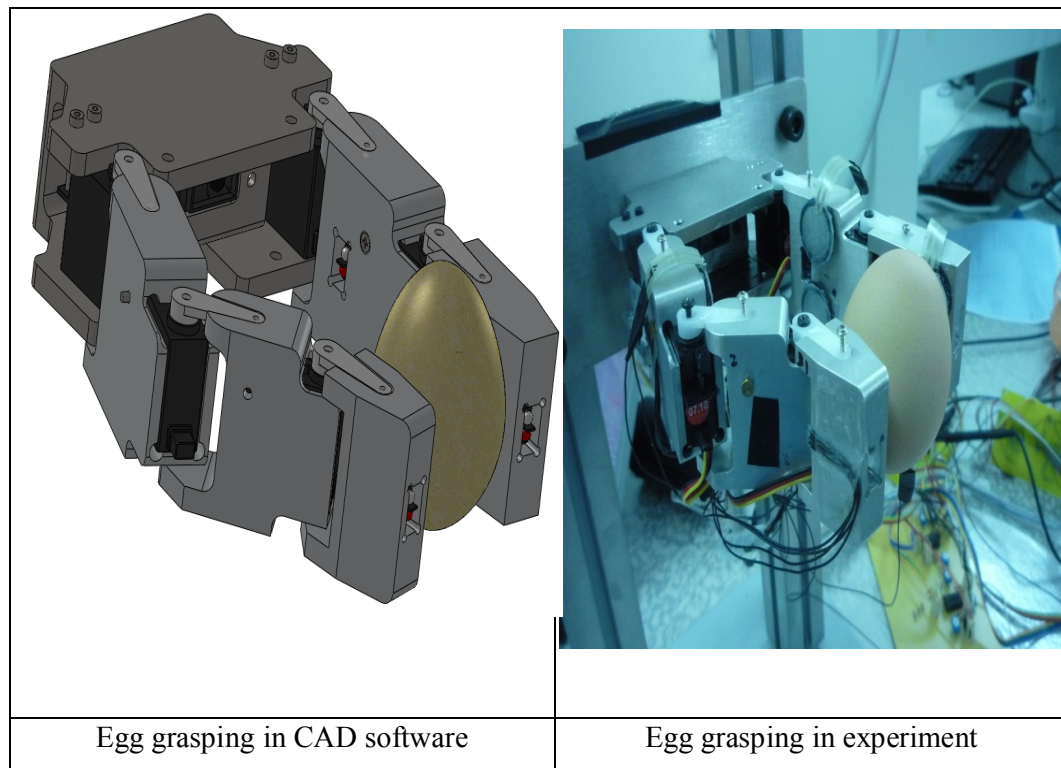


Figure 6.1: Comparison between simulated grasping pattern and the experimental grasping pattern

Discussion

The grasping patterns of the gripper in figure 6.1 are same as the simulated pattern in SolidWorks. This has shown that the fabricated gripper is able to perform the grasping pattern as simulated in the CAD software without much difference.

6.2.1.1 Experiment on spring

Table 12: Experiment result on spring

Force applied (N)	Elongation relative to X0	k (N/m)
0	0	0
0.05	0.01	5
0.1	0.02	5
0.15	0.03	5
0.2	0.04	5
0.25	0.05	5

The spring used in the experiment of obtaining the force at the tip has the constant of 5N/m. This constant will be used in experiment on maximum force at tip.

Table 13: Force experiment result on finger thumb

	Spring elongation (mm)	Experimental Value of Force Respond, Newton, (N)	Percentage error (%)
Experiment 1	43.0	0.215	3.327
Experiment 2	42.0	0.210	5.535
Experiment 3	43.0	0.215	3.327
Experiment 4	42.0	0.200	5.535
Experiment 5	44.0	0.220	1.079
Average value	42.8	0.214	3.760

Calculation

Now, taking the equation in (28), substitutes 1n_1 with the maximum torque which is the stall torque of the servomotor given in the datasheet. The length of l_1 , l_2 and l_3 is 0.35m, 0.40m and 0.53m. The degree of θ_3 and θ_2 is assumed to be 90° because only joint 3 will turn while joint 2 and joint 1 will remain in same position.

$${}^1n_1 = l_3 f_y + l_2 (f_x S_3 + f_y C_3) + l_1 (f_x C_3 S_2 - f_y S_3 S_2 + f_x S_3 C_2 + f_y C_2 C_3)$$

$$0.1172 = 0.35 f_y + 0.4 (f_x * \sin(90) + f_y \cos(90)) + 0.35 (f_x * \cos(90) * \sin(90) - f_y * \sin(90) * \sin(90) + f_x * \sin(90) * \cos(90) + f_y * \cos(90) * \cos(90))$$

$$f_x = 0.875 f_y \quad (45)$$

Now, forming the second equation at 2n_2 ,

$${}^2n_2 = l_3 f_y + l_2 (f_x S_3 + f_y C_3).$$

$$0.1172 = 0.35 f_y + 0.4 (f_x * \sin(90) + f_y * \cos(90))$$

$$0.1172 = 0.35 f_y + 0.4 * 0.875 f_y$$

$$f_y = 0.167428 \text{N} \quad (46)$$

Now substitute (46) into (45)

$$\begin{aligned} f_x &= 0.875 * 0.167428\text{N} \\ &= 0.146499 \end{aligned}$$

The total force of the finger gripper at the tip:

$$\begin{aligned} F_T &= \sqrt{0.167428^2 + 0.146499^2} \\ &= 0.2224\text{N} \end{aligned}$$

The percentage error of the calculated value and the experimental value,

$$\frac{(0.214 - 0.2224)}{0.2224} \times 100\% = 3.776\%$$

Discussion

When the link of gripper's finger is long, the reaction force at the finger's tip will be low. This is due to the moment of force which the equation is:

$$M = F * L$$

Where

M = moment force or torque

F = force

L = length

Given the moment is fixed; the force will decrease as the length increased. The force can only be increased if L is shortened or torque is changed to high.

Conclusion: The force at the tip is verified to have 0.214N.

6.3 Sensors Development

6.3.1 Experiment on Location of Sensors

Objective: Determine the best location of the infrared sensors to have wide and effective area of sensing.

Hypothesis: Locating the sensors to the end of the gripper's finger will increase the width of the effective sensing area of the infrared sensors.

The locations of infrared object detector on the gripper's fingers are first calculated using the equations which have been formulated. Three sets of locations of the sensors are chosen which is near the end of the gripper's finger's tip and thumb. The calculation results of area sensing using Beyer formula are compared with the simulated result as shown in Table 14 and Table 15.

Table 14: The calculated area of sensing of the Infrared sensors relative to the location chosen

Location of sensors	Distance of the IROD sensors relative to joints (mm)		
Tips (Joint 1)	22.83	20	10
Finger link 3 (Joint 3)	22	20	10
Finger link 5 (Joint 5)	21.4	20	10
Thumb (Joint 4)	24	20	10
Resulted Area(mm^2)	3906	3785.946	3077.875

Table 15: The simulated area of Sensing of the Infrared Sensors relative to the location chosen

Location of sensors	Distance of the IROD sensors relative to joints (mm)		
Tips (Joint 1)	22.83	20	10
Finger link 3 (Joint 3)	22	20	10
Finger link 5 (Joint 5)	21.4	20	10
Thumb (Joint 4)	24	20	10
Resulted Area(mm^2)	3750	3585	2879

The distance chosen in Table 14 is the distance of the infrared object detector relative to the corresponding joints. For example, the distance of 22.83mm of IROD at tips is the distance measured away from the joint 1. The corresponding joints are shown in figure 6.2.

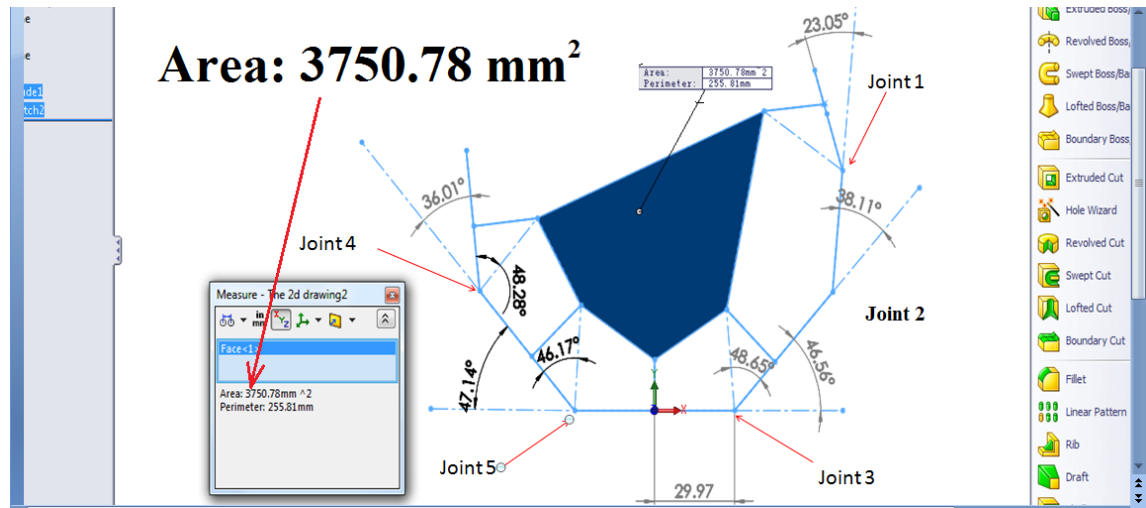


Figure 6.2: The maximum effective sensing area of the IROD and IRDD simulated in SolidWorks

Discussion

Having the IROD placed near the end of finger tip will increase the effective sensing area as shown in Table 15. The highlighted blue area in figure 6.2 is the sensing area which will be covered by all the infrared sensors. This is area will be the position of the object to be sense and if this area is wide, the size of the object can be detected is bigger.

However, the sensing area is also affected by the movement of the gripper's and its length. If the gripper's finger is short, the sensor location will be short and this will affect the maximum effective sensing area. The sensing area will be bigger if the open the fingers wide.

Conclusion: The maximum effective sensing area can be obtained by placing the infrared sensors at the end of the gripper's finger. Hypothesis is proven.

6.4 Servomotor's angle's of turning relative to the IROD detection range on the object's surface

Objective: Compare the actual position of the servomotor during the detection of the object relative to the Infrared Object Detector's sensing with the simulation in CAD software.

Hypothesis: The actual position of the servomotor should be the same as the simulated result given that no external disturbance occurred.

Table 16: Experiment on servomotors' angle of turning relative to IROD's detection on different object's position at dim room

Distance from base (cm)	Servomotor's Angle of Turning Degree				
	θ_1	θ_2	θ_3	θ_4	θ_5
1.5	143	100	65	81	110
2	135	101	72	78	120
2.5	135	90	65	88	115
3	125	80	65	92	115
Average	134.5	92.75	66.75	84.75	115

Table 17: Simulated of Servomotor's angle of turning relative to IROD's detection on different

Distance from base (cm)	Servomotor's Angle of Turning Degree (θ)				
	θ_1	θ_2	θ_3	θ_4	θ_5
1.5	145.09	102.87	63.7	79.23	118.6
2.0	137.59	103.06	70	76.39	120.94
2.5	133.43	97.12	65	86.1	117.28
3.0	129.29	92.97	65	88.47	114.9
Average	136.35	99.005	65.925	82.5475	117.93

Discussion

Comparing the angles between Table 16 and Table 17, the actual angle of the servomotor in experiment is close the simulation in SolidWorks. The slight difference is due to the turning degree of the servomotor which controlled by the input signal from control system.

The servomotor's degree of turning is 1.86 degree per instruction due to the control resolution is governed by Real Time Clock (RTC). This means when the IROD detected the object which needs only 0.5 degree of turning from the servomotor, the servomotor cannot perform such action because it can only move 1.86 steps on each time due to the signal waveform from dsPIC. This resulted on slight difference of angle detection in experiment without the external disturbance.

Conclusion: The gripper's servomotor angle of turning is highly dependent from the signal of IROD. Besides that, the control signal from the dsPIC to the servomotor can affect its turning position's accuracy.

6.5 Force Sensor's Development

6.5.1 Experiment of Force Applied on Specimen

Objective: To obtain the point of limit force on each of the selected specimen.

Hypothesis: Three objects which are can, pen and egg represent the elastic, rigid and brittle object has different breaking point of force.

6.5.1.1 Force Experiment on Can

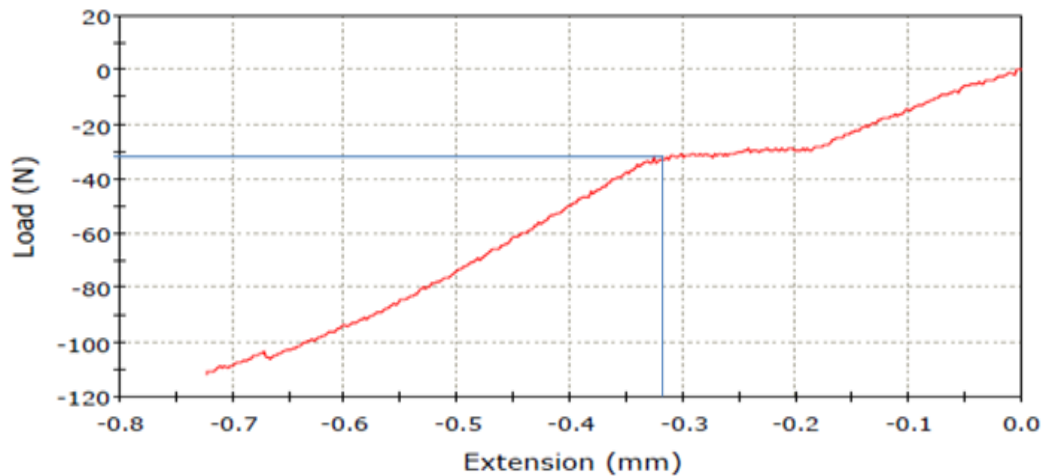


Figure 6.3: Experiment on can subjected to different loads.

The deformation point of the can shown in figure 6.3 is around 30N which the compression limit is 0.3mm. From the applied force of 0N to 30N of compression, the can experience the elastic deformation in which the can's surface can return to original shape if force is removed. At constant 30N, the compression of the can did not change due to the resistance from the structure of the can itself. After the compression of around 0.3mm, the can experience plastic deformation in which the can structure will not offer any resistance. At this point, the shape will not return to original shape after the force is removed.

6.5.1.2 Force Experiment on Pen

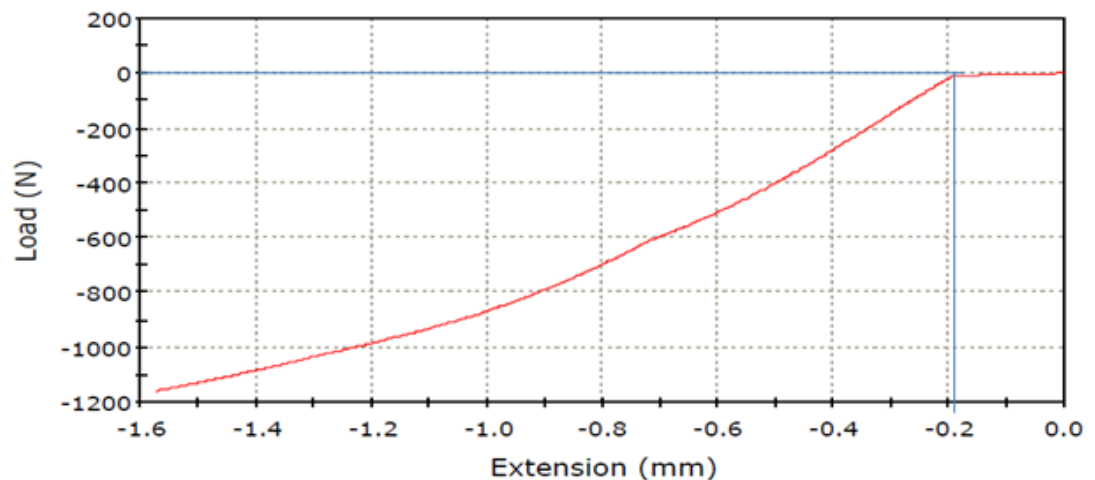


Figure 6.4: Force Experiment on Pen Subjected to Different Load

The plastic pen did not offer any elastic deformation as shown in figure 6.4 due to its rigid structure. The plastic deformation rate is 30N on each 0.1 mm. This indicates the structure of the pen is rigid and strong in which it can offer very high force resistance compare to others.

6.5.1.3 Force Experiment on Eggs Subjected to Different Load

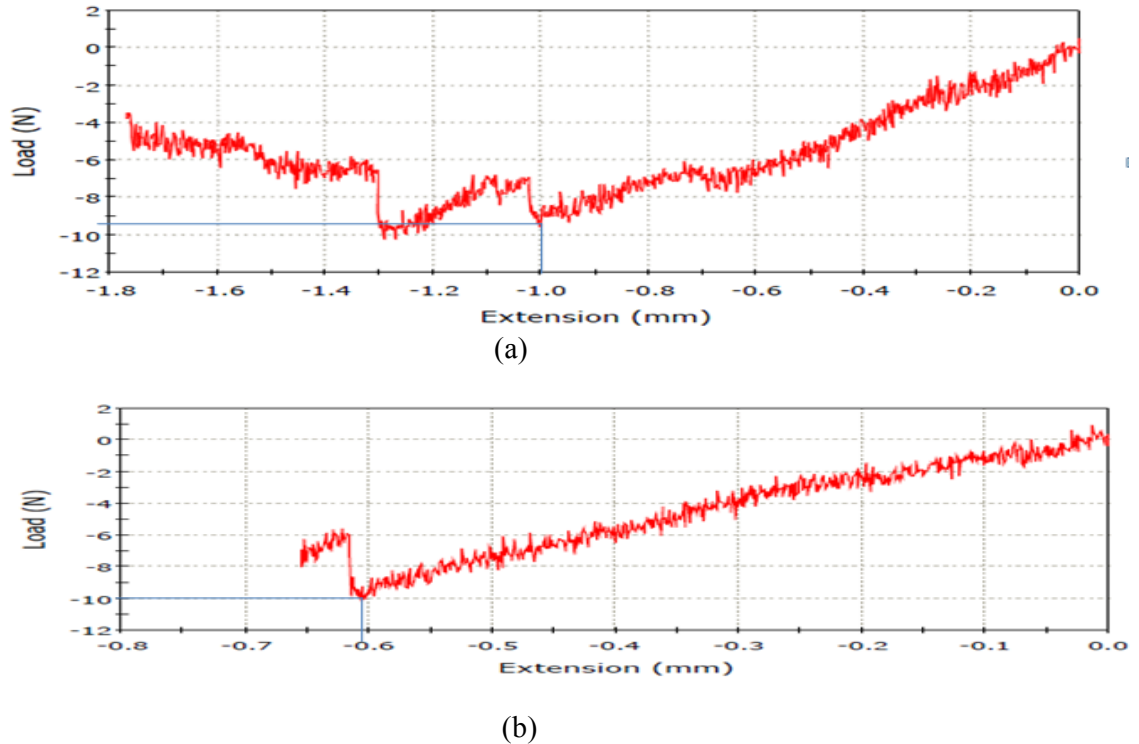


Figure 6.5: The deformation of different egg in (a) and (b) subjected to different load.

The experimented breaking points for the eggs are observed to be around 10N with the compression of 0.6mm which is very short. The graph in figure 6.5 (a) experienced a bounce at yield point of 1mm due to the breaking surface of the egg. The egg's surface experiences a complete plastic deformation at 1.2mm compression. In graph (b), the breaking point is also 10N at 0.6mm. The compression limit for the egg in (b) is lower than the graph (a) and this indicates that the egg's compression limit is around 0.6mm to 1mm at 10N.

Conclusion: The breaking point of tin is around 30N with elastic deformation, pen is 30N with instantaneous plastic deformation and egg has average of 9N of plastic deformation. Each of the objects' force response has been obtained.

6.5.2 Experiment on Force Sensors

Objective: Determine the force respond of the FSR which the area of sensing is reinforced with rubber pad.

Hypothesis: The force sensing sensitivity of the FSR which has been attached with the rubber pad will be higher than sensing sensitivity stated in data sheet

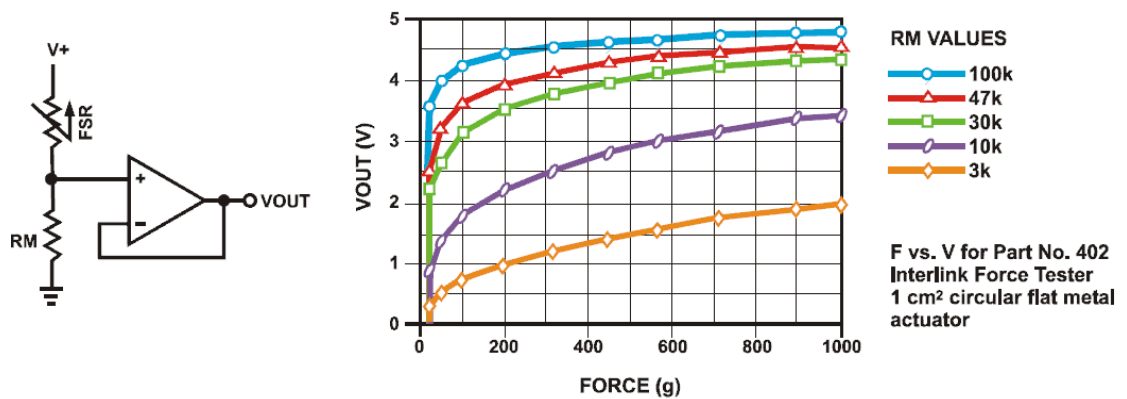


Figure 6.6: The sensing sensitivity using 10k ohm as RM values on the actual Force Sensing Resistor from data sheet (Adopted from Interlinks Electronics, 2011)

Table 18: Experiment of Force Sensor Resistor on Different Load

FSR	Load (gram)												
	30	40	50	60	70	80	90	100	110	120	130	140	150
1	0.33	0.6	1.04	1.21	1.45	1.72	1.86	1.98	2.18	2.25	2.38	2.43	2.56
2	0.46	0.88	1.2	1.85	2.05	2.31	2.53	2.65	2.73	2.93	2.86	2.92	3.04
4	0.42	0.8	1.3	2.05	2.01	2.14	2.45	2.46	2.65	2.72	2.86	2.92	3.12
7	0.29	0.44	0.85	1.03	1.27	1.46	1.55	1.71	1.81	1.86	1.99	2.08	2.14
8	0.91	1.22	1.65	1.83	1.98	2.17	2.28	2.4	2.59	2.67	2.82	2.87	2.98
AVERAGE	0.48	0.78	1.20	1.59	1.75	1.96	2.13	2.24	2.39	2.48	2.58	2.64	2.76

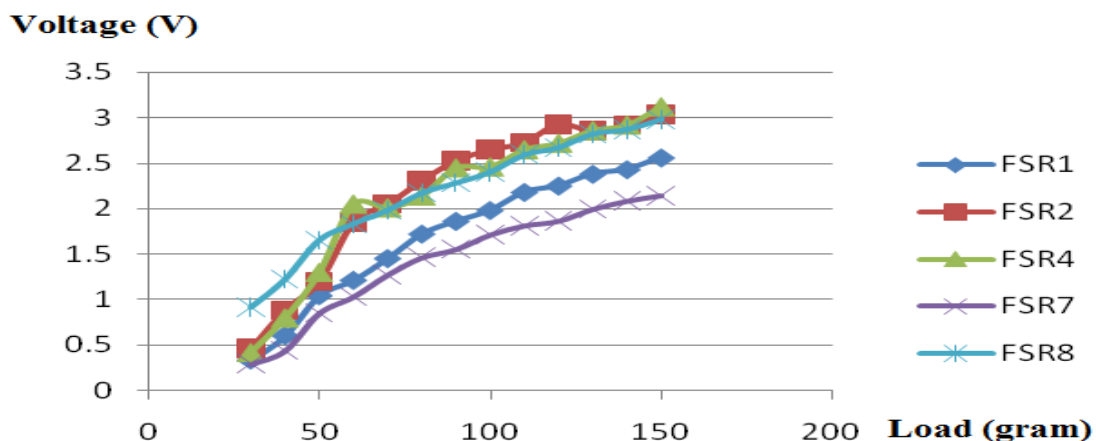


Figure 6.7: The experimented sensing range of FSRs which the sensing area have been attached with rubber pad

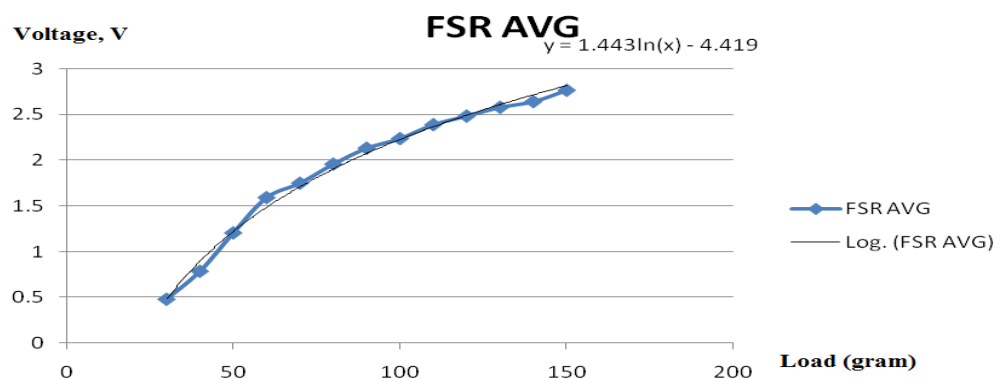


Figure 6.8: Average force respond corresponding to voltage output which is relative to load applied

Discussion

The result from data sheet shown in figure 6.6 has the maximum voltage output of 2.7V at 570 gram. Comparing the figure 6.6 and figure 6.7, the sensing range of all FSR which is reinforced with rubber pad has been increased where the maximum voltage output at 150 gram is in between 2.0V and 2.7 V and the minimum is 35 gram which is around 0.5V.

$$P = \frac{F}{A}$$

Where,

P = pressure

F = force

A = area

This is due to the equation above where FSR attached with rubber pad has decrease the sensing area and diverts all the force into a small area to increase the pressure. When the pressure is increased, the voltage will increase correspond to the increase of resistance of the FSR. The reason of putting the rubber pad is because the egg force respond is 10N which is very low. This needs a high sensitivity FSR to detect such small force

Conclusion: The rubber pad attached to the sensing area can increase the sensitivity of the force sensors via voltage output at small applied force.

6.5.3 Force Respond on Each Location of the FSR

Objective: Determine the number of force respond of Force Sensing Resistor and their force respond level at different point of the gripper's finger.

Hypothesis: The force respond from the FSR which locates further from the palm joint (joint 3 or 5) will be much lower than the FSR near the palm's joint due to the torque at the finger tip is much lower than the palm's joint.

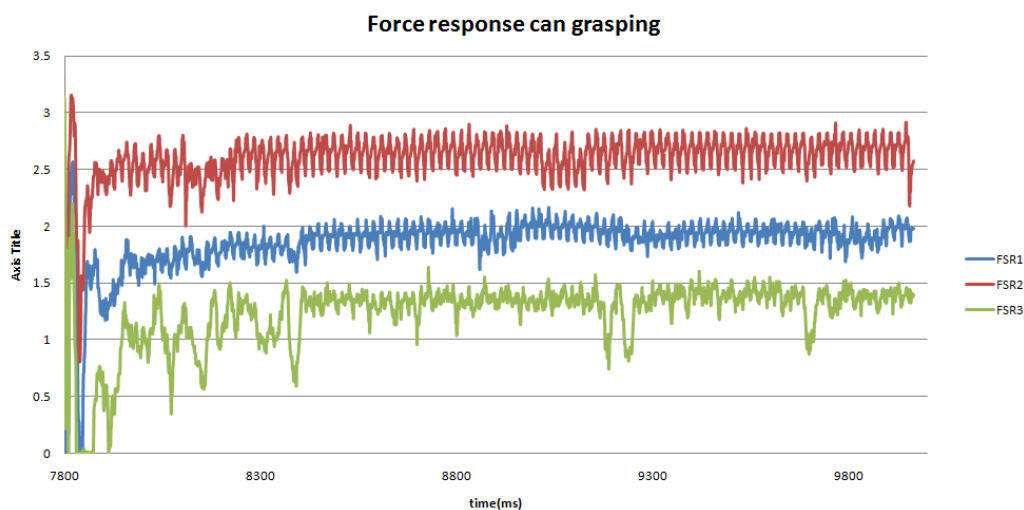


Figure 6.9: Force response on FSR when grasping a can

One of the sample specimens which are the can is used to grasp with the gripper mounted with force sensors. There are 3 force respond obtained from the force sensors which made contact. The voltage output from these force sensors will be applied into the equation in the figure 6.9.

$$Y=1.443\ln(X)-4.419$$

Where:

X = force respond in gram

Y = voltage output from the experiment

The result of the force respond on each of the sensor is shown in Table 19.

Table 19: The force sensors output voltage and force respond on can grasping

Force sensor	Location	Output voltage, V	Force respond, N
1	30mm distance from the joint 2	2.0	0.08
2	25 mm distance from the joint 3	2.7	0.138
3	30 mm distance from the joint 5	1.4	0.560

Discussion

In Table 19, the force respond from the FSR 2 is the highest due to its location which is near to the driving joint 3 at the palm. The joint 3's torque is the main driving source and it is used to determine the overall force applied at each of the finger location.

Other than that, the figure 6.9 shows that each of the force respond has critical damping when making contact with the object. This is due to the moment of inertia which is resulted from the impact of the gripper's finger body on the object's surface. The gripper's finger was bounce back when first contact was made and hit again with lower moment of inertia. This has caused a critical damping effect on the voltage output which corresponding to force responds.

The force respond from other FSR is 0 due to their location which is unable to make a contact with the object. For example, the force sensors at finger tip are unable to make a contact because the ends of gripper's finger tip unable to touch surface of the object.

Conclusion: The level of voltage output corresponding to the force respond is the highest at the finger near the joint 3

CHAPTER 7

DISCUSSION ON ENGINEERING DESIGN PROCESS

During the Engineering Design Process, the engineers from IPE Automation Sdn. Bhd. have recommended some changes to the design. This section will discuss on the changes made.

7.1.1 Pocket Hole

The edges of the pocket holes are recommended to be in radius shape.

Reason: This is due to the IPE recommendation that drilling the four holes first will allow the Computer Numerical Control (CNC) to drill the pocket hole easily. Furthermore, the holes at the pocket edges will offer no contact with the servomotor's edges as shown in figure 7.1. This will allow non collision between components. Other than that, the drilling bit of CNC unable to drill exact 90° sharp edges at the pocket hole.

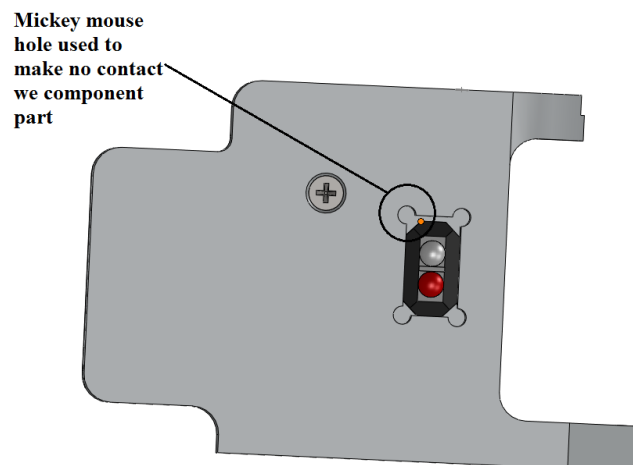


Figure 7.1: The Mickey Mouse hole drilled at the pocket holes

7.1.2 Bearing Housing

The bearing housing is located on the top of the surface of the finger body joint as shown in the figure 7.2 and figure 7.3. The initial design of the housing is located base of the finger's body. The IPE engineer has urged the housing to be relocated to the top surface.

Reason: It is better to have the housing hole on top surface of the finger body joint. This will allow the bearing to sit on the hole of the base rather than being 'hang' at the base of the finger's body. Furthermore, it is easy to be taken out by using any thin rod to take out the bearing as shown in figure 7.4.

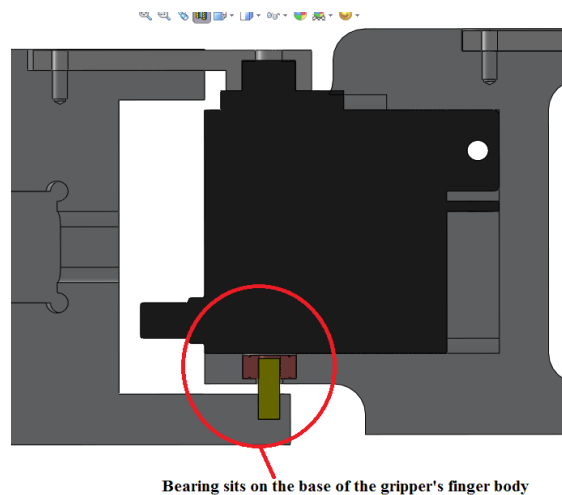


Figure 7.2: The new location of the bearing

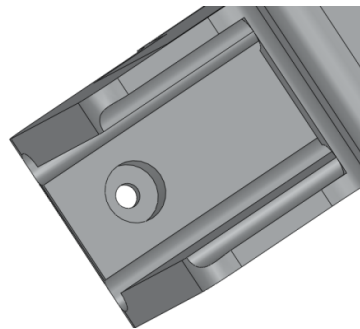


Figure 7.3: The new bearing housing location view in 3 Dimension.

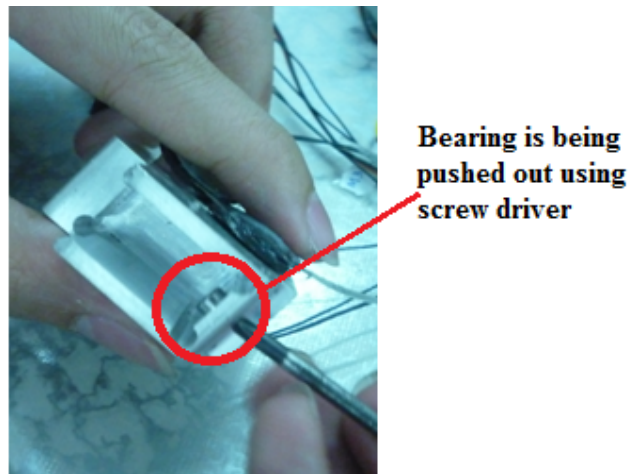


Figure 7.4: The bearing is pushed out with ease using a screw driver via base.

7.1.3 Palm

The usage of block material as raw material for the palm is recommended by IPE.

Reason: This is due to fact that the plate bending operation requires the plate thickness to be low in order for the machine to bend an accurate 90° angle. Due to the wall thickness of the designed palm is out of the bending machine's specification, the block shape raw material is used. The removal of the block shape internal material into 'U' shape is done by drilling it using CNC machine.

7.1.4 Screw hole

The screw hole needs to be reassigned with specific hole.

Reason: The screw holes are normally drilled with a set of value using industrial standard. This is to accommodate the existing screw dimension in the market.

The screw holes on each of the gripper finger and the palm is recommended to follow the industrial standard. The screw holes recommended was M3 flat head, M2 oval head and M3 Tap Drill. The 'M' indicates the size of screw used and the number 3 indicates the size is 3mm. Figure 7.5 shows one of the M2 Flat Head holes.

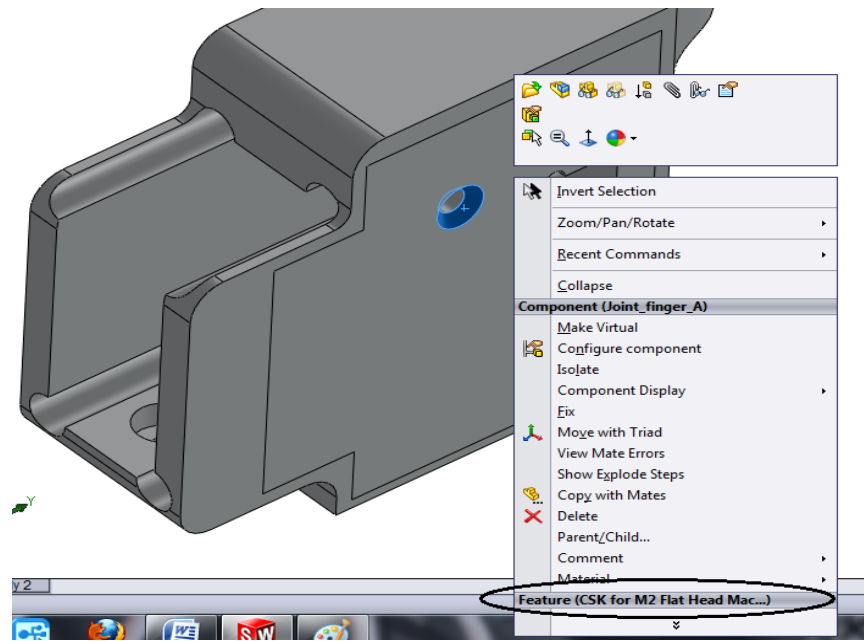


Figure 7.5: The CSK screw hole that support the servomotor with finger body

7.1.5 CAD Drawing

The CAD drawing dimension is needed to be readjusted, especially the dimension which is important as shown in figure 7.6.

Reason: Figure 7.6 shows the two ‘U’ shape palms with side view. The dimension labelling for the right palm is wrong. The middle opening of the palm is the most important dimension because the mechanical components will be inserted into it. The IPE has urged the proper labelling as shown in palm at the right side where the opening is labelled with exact 24mm dimension. This is to ensure the miller will mill the middle hole at 24mm exactly. If the dimension is label as shown at left palm, the miller might think the middle part is important and the middle part’s dimension will be milled with tolerance.

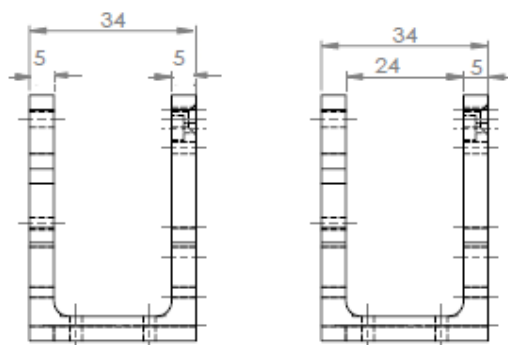


Figure 7.6: Two ‘U’ shape palm with different labelling

7.1.6 Dowel pin.

The dowel pin should be custom made with slight angle at the tip rather than purchase it in the market.

Reason: The dowel pin with angle will give the ease of slot in the dowel pin into the bearing and hole. The dowel pin in the market is mainly in a straight thin rod. This is because when the dowel pin is manufactured, it is made in mass quantity. Furthermore, the straight thin rod is set to be standard form in industrial level. However, this straight thin rod type is difficult to be inserted into the hole of any object due to edge that will block the insertion. The dowel pin used in this project has an angle to let the bearing to be inserted with ease.

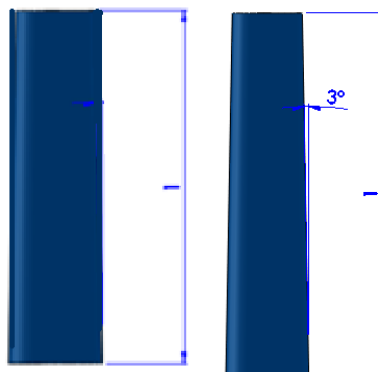


Figure 7.7: The thin rod dowel pin on the left side and the dowel pin with angle on right side

The reason of pocket at palm is being drilled 35mm into the body is due to the IRDD characteristic. As shown in figure 7.8 IRDD SHARP GP2D120 has a characteristic in which it can only sense accurately at 4cm distance or further. When the object's position has falls below 4cm or too near to the IRDD, it will not able to detect the distance of the object precisely. Therefore, the IRDD needed to be offset from the base gripper line. The offset also allows IRDD to sense object as close range.

7.1.1 IRDD sensors location and offset in palm

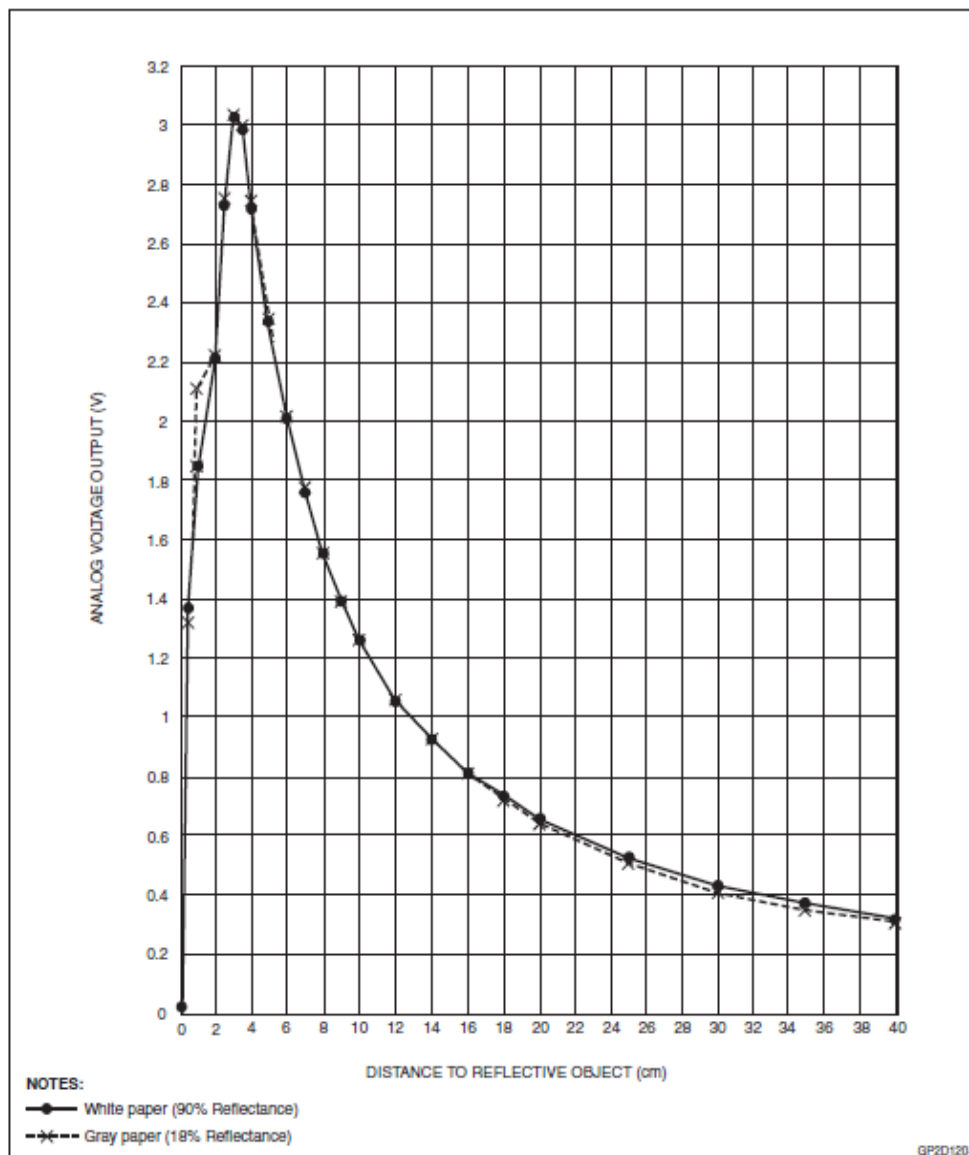


Figure 7.8: Infrared Distance Detector's voltage output relative to distance sensing.

7.1.2 Gripper's finger Vibration

The gripper's finger vibration has occurred during the movement of the servomotor. The vibration is due to the moment of inertia of the finger's body mass resisting the changes in rotation. When the gripper's finger move, the moment of inertia is created at the finger body and when the gripper's finger stop, the moment of inertia is transmitted to the part that stops first which is the gear. This make the gear prunes to wear and tear.

In solving this problem, the turning speed of the servomotor is slowed down in order to lower the moment of inertia. This will ease the stress on the gear. Slowing down the servomotor indeed will decrease the force and torque because the speed is controlled by the input signal. If the number of input signal at one period is high, the force and torque will low. Therefore, the speed of servomotor rotation at beginning is made to slow and when the gripper's finger touches the object's surface, the servomotor will be fed with high numbers of input signal to increase its torque.

7.1.3 L-shape plate to fix position

The servomotor will run out of position on each time it rotates. This is due to the inertia of the gripper's finger which drags the servomotor out of its position. The servomotor in will be added with the L shape plate to fix its position. This will fix the servomotor from run out of position on each time it moves.

L-shape plate used to fix the servomotor's position.

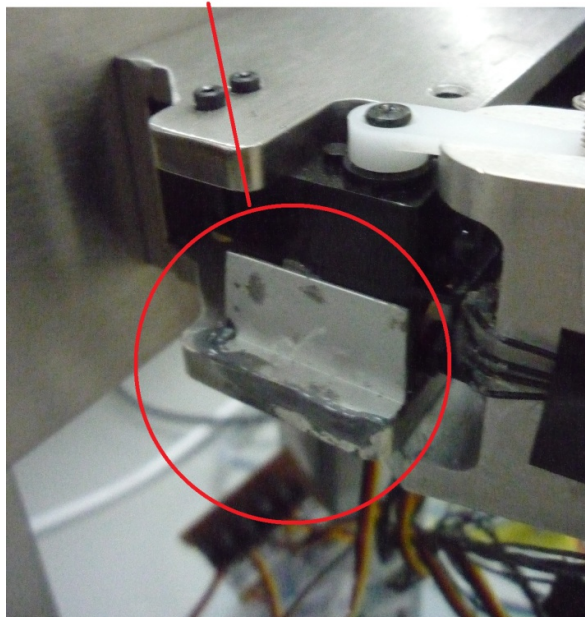


Figure 7.9: The L-shape fix at the side of the gripper's finger

7.1.4 Position of Force Sensor

The force sensors are attached at the middle of the link as shown in the figure 7.10. When the object is gripped, the applied forces will be distributed on the surface of the gripper finger. We take the middle point of each link to record the force. The force sensor cannot be attached near the joint.

Reason: This is due to the rotation between two links at the joint will block the force sensor from being pressed against the surface of the object as shown in figure 7.11.

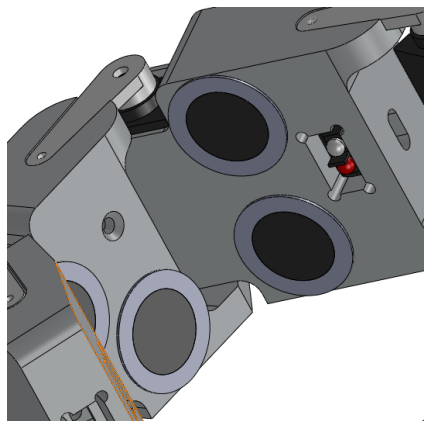


Figure 7.10: The force sensors are attached at the middle of the finger body.

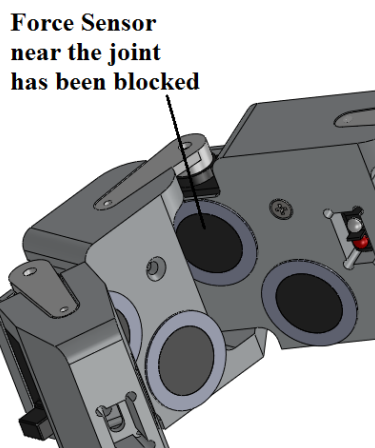


Figure 7.11: The force sensors are blocked by the joint

7.1.5 Offsetting the position of IRDD into the palm

The IRDD sensing range is 4cm and above. Any object falls below 4cm or too near to the IRDD will causes the sensing of IRDD to fail. This is because the wavelength from the emitter can only be reflected to the receiver at 4cm or further. An offset method which locates the IRDD into the gripper palm by 3.5cm has been done by drilling the pocket at the gripper's base to accommodate the extruded PCB board. This method can shorten the reflecting point from the base of the gripper. Figure 7.12 shows the idea of offsetting the IRDD. The figure 7.13 shows the IRDD offset in assembly.

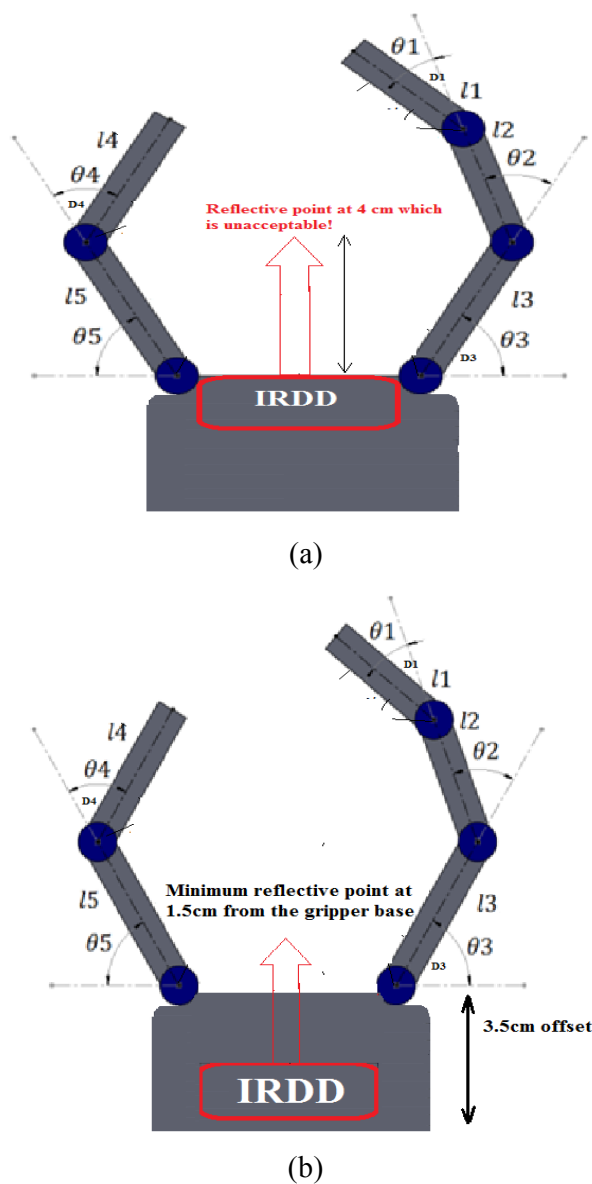


Figure 7.12: The reflective point of the IRDD at 4cm from the base and new reflective point at 1.5cm from the base by offset the IRDD into gripper.

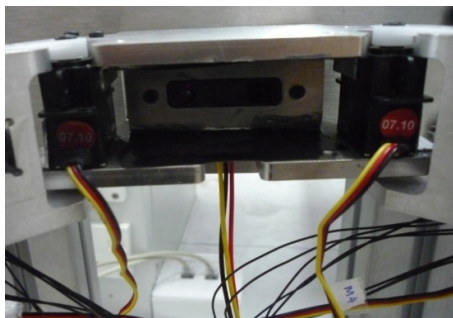


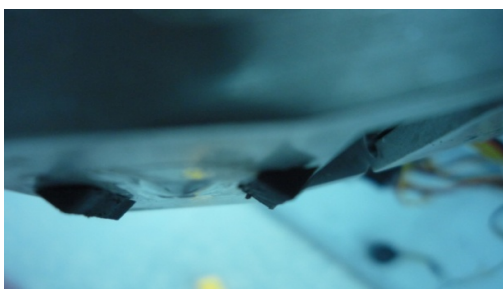
Figure 7.13: The IRDD offset 35mm into the palm body

7.1.6 The Grasping at Finger Tip Subjects to Rotational Force

The IVOARM is a gripper with two fingers. Unlike the gripper with 3 fingers, the gripping at finger tip will be difficult due to the rotational force. The rotational force is the body of the object rotates while being gripped. A solution has been done by putting two layer of straight triangle pad as shown in figure 7.14.



(a)



(b)

Figure 7.14: (a) The straight pad stacked at the finger tip. (b) Top view which shows the pad is in triangle shape.

7.1.7 Publication in symposium

At the end of this project, the project team has submitted a symposium paper to IEEE 6th International Symposium on Embedded Multicore SoCs (MCSocS-12) in Japan. The paper has been attached with the thesis.

CHAPTER 8

CONCLUSION AND RECOMMENDATIONS

8.1 Conclusion

As the conclusion, the IVOARM gripper has achieved the following objectives:

8.1.1 Mechanical Design

IVOARM has been designed and fabricated to host multiple sensors. The IVOARM has flexible fingers in terms of number of degree of freedom and its angle of rotation must be independent from others. The force at the finger tip has been verified.

8.1.2 Sensors Development

1. Infrared Sensors Development

The infrared sensors have been placed at the suitable location on the IVOARM gripper's finger. The angle of turning accuracy of IVOARM's joint relative IROD is high.

2. Force Sensor Development

The force limit on each of the specimens which is elastic, brittle and rigid has been obtained. The force sensors' sensitivity used in IVOARM has been reinforced and its output characteristic has been obtained. The force sensors' response relatives to position during gripping a specimen have been studied.

8.2 Recommendation

8.2.1 Dynamic Force Control

The IVOARM gripper can be used to implement the dynamic force control. The dynamic force control is used to control the amount of force applied to the object's surface given the surface of the object is soft or hard. The Dynamic Force Control can be implemented using Lagrange method or Euler-Newton Iterative method in dynamic force.

8.2.2 Slip sensing

The slip sensing can be implemented together with the dynamic force control. The force sensors are stacked into two rows as shown in figure 8.1. The voltage generated from the pressure on the force sensor will be used as feedback to force control system. If the object's slip occurred, the difference of pressure between this two force sensors will prompt the force control system to apply more pressure on it to stop the slip.

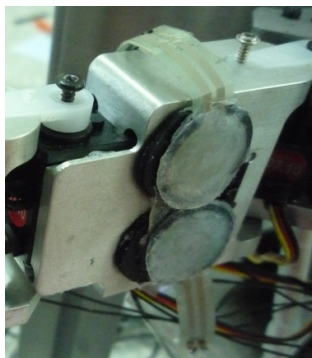


Figure 8.1: The force sensors stacked in two rows

8.2.3 Determine the Volume of the object

The polygon area equation used to determine the positions of the sensors can be developed to find the area of the object's surface. This can be done by determine the object's area within the boundary grasped by gripper's finger. Furthermore, if the gripper is attached to the robotic arm, it can be used to scan the height of the object using the infrared object detector. This height can be multiply with the area of the gripper's gripping boundary to search the volume of the object gripped.

8.2.4 Torque Increment

The servomotor used in the future should have high torque, especially the servomotor at the Joint 3 and Joint 5. The torque to drive the gripper's finger is governed by the servomotor at Joint 3 and Joint 5. The servomotors at other joints are used to fix the shape of the finger. Other than that, the force of the gripper's finger tip is governed by the torque at the Joint 3 and Joint 5.

8.3 Precaution

8.3.1 Servomotor

The servomotors which used to drive the gripper's finger are prone to tear and wear. The tear and wear is not on the servomotor itself but the gear inside. The gear which is currently being used in the servomotor is heavy duty resin type. The gear teeth are easily to be wear and tear if external forces are applied on it. The gear of servomotors used in the future must be metal form which is prone to the external force. Other than that, the gripper's finger is not allowed to rotate with hand at high speed. It will damage the teeth of the gear.

8.3.2 Wiring

The wiring connection between the circuit board and the IVOARM gripper is too many and needed to be rearranged. If the wiring is not arranged, it might cause accident if one of the wire's connectivity is broken.

8.3.3 Complete wiring connection between IVOARM and circuit board.

It is reminded that the cable between IVOARM and circuit board must be full connected before switch on the power. It is learnt that the IVOARM gripper's finger will went to hay wire and hit the Foundation Settlement when the servomotor is not connected to dsPIC.

REFERENCES

Blais, François; Beraldin, Jean-Angelo; Cournoyer, Luc; El-Hakim, Sabry; Picard, Michel; Domey, Jacques; Rioux, Marc, (2001) The NRC 3-D Laser Tracking System: IIT's Contribution to the International Space Station Project, Proceedings of the 2001 Workshop of Italy-Canada on 3D Digital Imaging and Modeling Application of Heritage, Industry, Medicine, & Land. Padova, Italy April 2001, Retrieved on March 3, 2011 from

<http://nparc.cisti-icist.nrc-cnrc.gc.ca/npsi/ctrl?action=rtdoc&an=9183288&lang=en>

Mr Goh Han Cheong, IPE Company Director, August 4, 2010

Northern Digital Industry (2010) "Machine Vision Technology," NDI website. Retrieved on March 3, 2011 from <http://www.ndigital.com/medical/technology-machinevision.php>

Anders Hagnelius , Supervisor Cs-umu , Niclas Börnin, (2004) Visual Odometry, CVPR IEEE Computer Society, 652-659, Conference on Computer Vision and Pattern Recognition, Retrieved on March 3, 2011 from <http://citeseerx.ist.psu.edu/viewdoc/summary?doi=10.1.1.109.6039>

Zaki, A.M.; Soliman, A.M.; Mahgoub, O.A.; El-Shafei, A.M.; (2010) High performance robotic gripper based on choice of feedback variables, Information and Automation (ICIA), 2010 IEEE International Conference on Conference on Digital Object Identifier: 10.1109/ICINFA.2010.5512336 , 54-59 Retrieved March 21, 2011 from

<http://ieeexplore.ieee.org.libezp.utar.edu.my/stamp/stamp.jsp?tp=&arnumber=5512336>

Christophe Leroux, et al, (2007) Robot Grasping of Unknown Objects, Description and Validation of the Function with Quadriplegic People, Proceedings of the 2007 IEEE 10th International Conference on Rehabilitation Robotics, Retrieved March 21, from <http://ieeexplore.ieee.org.libezp.utar.edu.my/stamp/stamp.jsp?tp=&arnumber=4428403>

Daft, Richard L. (2008) The New Era of Management. Retrieved April 1, 2011 from <http://www.pdf4me.net/pdf-data/richard-l-daft-new-era-of-management--edition.php>
Jun Hee Lee (2002) The General Specification of HS-56HB, Retrieved April 1, 2011 from <http://www.rctoys.com/pdf/hitec-servos/HIT-HS56.pdf>

Eric Weisttein (2011) Polygon Area, Wolfram Mathworld. Retrieved from <http://mathworld.wolfram.com/PolygonArea.html>

Interlink Electronics (2011) Force Sensing Resistor Integration Guide Evaluation Part Retrieved, Massachuschet Institute of Technology. Retrieved March 21 from <http://www.media.mit.edu/resenv/classes/MAS836/Readings/fsrguide.pdf>

SHARP (2006) GP2D120 Optoelectronic Device, SharpSMA. Retrieved March 20 from www.sharpsma.com/webfm_send/1205

Visha (2009) TCRT 5000, Reflective Optical Sensor with Transistor Output, Vishay Intertechnology Asia Pte. Ltd. Retrieved March 21, 2010 from <http://www.vishay.com/docs/83760/tcrt5000.pdf>

APPENDICES

APPENDIX A: The CAD drawing parts.